

**UNIVERZITA KARLOVA V PRAZE
FARMACEUTICKÁ FAKULTA V HRADCI KRÁLOVÉ
KATEDRA ANALYTICKÉ CHEMIE**

**VYUŽITÍ NANOKOMPOZITŮ
JAKO POVRCHŮ PRO SALDI-MS**

DIPLOMOVÁ PRÁCE

2010

Eva Böhmová

**CHARLES UNIVERSITY IN PRAGUE
FACULTY OF PHARMACY IN HRADEC KRÁLOVÉ
DEPARTMENT OF ANALYTICAL CHEMISTRY**

**NANOCOMPOSITES AS SURFACES
FOR SURFACE-ASSISTED
LASER DESORPTION/IONIZATION
MASS SPECTROMETRY**

GRADUATION THESIS

2010

Eva Böhmová

Prohlášení

Prohlašuji, že tato práce je mým původním autorským dílem. Veškerá literatura a další zdroje, z nichž jsem při zpracování čerpala, jsou uvedeny v seznamu použité literatury a v práci řádně citovány.

Supervisors:

Assoc. Prof. Leopold L. Ilag, Ph.D.

Department of Analytical Chemistry
Stockholm University
Arrhenius Laboratory of Natural Sciences
S-106 91 Stockholm
SWEDEN

Prof. RNDr. Petr Solich, CSc.

Department of Analytical Chemistry
Faculty of Pharmacy in Hradec Králové
Charles University in Prague
Heyrovského 1203, 500 05 Hradec Králové
CZECH REPUBLIC

ACKNOWLEDGEMENT

I would like to thank Professor Leopold Ilag, Doctor Mohammadreza Shariatgorji, and Doctor Zdeněk Spáčil for their time, their pieces of advice and help during my work on this thesis. I would like to thank Professor Petr Solich for his work on Erasmus program and his helpful comments concerning this work. I would like to thank Nina Aminlashgari for working with me on part of this project, for preparing the nanocomposites, and for discussing the results.

ABSTRACT

Matrix-assisted laser desorption/ionization (MALDI) is a soft ionization method used in mass spectrometry that is important for the analysis of biomolecules and large synthetic molecules. However, it is difficult to use MALDI for the analysis of small molecules because the matrix ions interfere with their analysis. Several surface-assisted laser desorption/ionization (SALDI) mass spectrometry methods have been developed as a solution to this problem. In this thesis, polylactide (PLA) nanocomposites containing halloysite nanoclay, hydroxyapatite, magnesium oxide, montmorillonite nanoclay, silicon dioxide, silicon nitride, titanium dioxide, and graphitized carbon black (GCB) nanoparticles were examined as surfaces for SALDI. The intensities of the signals of three human medicines: acebutolol, carbamazepine, and propranolol, obtained from these surfaces were compared to the signal intensities obtained from stainless steel MALDI plate without use of any matrix. The signal intensity was only enhanced when nanocomposites containing 30% GCB, 10% silicon nitride, and 10% titanium dioxide nanoparticles and analytes in concentration of 150 ppm were used. These results, together with the fact that PLA is a biodegradable polymer and can be obtained from renewable resources, make these materials potential environmentally friendly SALDI surfaces. The nanocomposite with 30% GCB nanoparticles has also been used for on-plate cleanup of a complex sample – human urine spiked with propranolol. Urine spot was washed with ammonia solution and subsequent SALDI analysis provided cleaner spectra where propranolol could be easily identified. Further work will be needed so that an easy and fast cleanup method prior to SALDI analysis using this surface could be refined.

ABSTRAKT

Ionizace laserem za účasti matrice (matrix-assisted laser desorption/ionization, MALDI) patří mezi měkké (šetrné) ionizační techniky hmotnostní spektrometrie a je důležitá zejména pro analýzu biomolekul a syntetických makromolekul. Použití MALDI pro analýzu nízkomolekulárních sloučenin je však obtížné, protože ionty matrice interferují s analýzou malých molekul. Jako řešení tohoto problému bylo vyvinuto několik metod, které využívají ionizaci laserem za účasti povrchu (surface-assisted laser desorption/ionization, SALDI). Předmětem výzkumu této práce byly možnosti využití nanokompozitů složených z polylaktidu a nanočástic halloysitu, hydroxyapatitu, oxidu hořečnatého, montmorillonitu, oxidu křemičitého, nitridu křemičitého, oxidu titaničitého a grafitizovaných sazí (graphitized carbon black, GCB) jako povrchů pro SALDI. Intenzity signálů tří léčiv, acebutololu, karbamazepinu a propranololu, získané z těchto povrchů byly porovnány s intenzitami signálů získaných bez použití matrice z nerezové destičky pro MALDI. Intenzita signálu byla zvýšena pouze, když byly použity tyto tři nanokompozity: nanokompozit s obsahem 30% GCB, nanokompozit s 10% nitridu křemičitého a nanokompozit s 10% oxidu titaničitého, a analyty v koncentraci 150 ppm. Díky tomu, že polylaktid je biodegradabilní a lze ho získat z obnovitelných zdrojů, dělají tyto výsledky z těchto materiálů potenciální povrchy pro SALDI šetrné k životnímu prostředí. Nanokompozit s obsahem 30% grafitizovaných sazí byl také použit pro vyčištění komplexního vzorku – lidské moči s přídavkem propranololu – přímo na daném povrchu. Kapka vzorku moči byla nanesena na povrch, vymyta roztokem amoniaku a následnou SALDI analýzou byla získána čistší spektra, kde byl propranolol snadno identifikován. Bude třeba provést další experimenty, aby mohla být vyvinuta rychlá a jednoduchá metoda pro vyčištění vzorku před SALDI analýzou s využitím tohoto povrchu.

CONTENTS:

1 INTRODUCTION.....	12
2 THEORY	14
2.1 MASS SPECTROMETRY	14
2.1.1 Mass Spectrometer.....	14
2.1.2 Matrix-Assisted Laser Desorption/Ionization.....	14
2.1.3 Matrix-Free Laser Desorption/Ionization Techniques.....	16
2.1.4 Time-of-Flight Analyzer.....	19
2.1.5 On-Plate Sample Cleanup.....	20
2.2 POLYLACTIDE NANOCOMPOSITES	21
2.2.1 Polylactide	21
2.2.2 Nanocomposites.....	23
2.3 DEFINITION OF TERMS	24
2.3.1 Signal-to-Noise Ratio	24
2.3.2 Partition Coefficient.....	24
3 EXPERIMENT	25
3.1 CHEMICALS, MATERIALS AND SAMPLES	25
3.1.1 Water.....	25
3.1.2 Standards.....	25
3.1.3 Other Chemicals	26
3.1.5 Nanocomposites.....	26
3.1.4 Urine	28
3.2 INSTRUMENTATION.....	28
3.2.1 Mass Spectrometry	28

3.2.2 Software	28
3.3 DATA GATHERING.....	29
3.3.1 Sample Spotting.....	29
3.3.2 Data Collection	30
3.3.3 On-Plate Sample Cleanup.....	30
4 RESULTS AND DISCUSSION	31
4.1 METHOD DEVELOPMENT	31
4.2 COMPARISON OF SURFACES	32
4.2.1 Comparison of Nanocomposites Using 150 ppm Analyte Solutions	32
4.2.2 Comparison of Nanocomposites with Different Amounts of Nanoparticles..	35
4.2.3 Comparison of Nanocomposites Prepared Using Different Techniques	37
4.2.4 Comparison of Different Concentrations of Analytes on MALDI Plate	39
4.2.5 Comparison of Nanocomposites Using 10 ppm Analyte Solutions	42
4.4 “HOT SPOTS” PROBLEM	46
4.5 ON-PLATE SAMPLE CLEANUP	48
4.5.1 Sample Cleanup on Nanocomposite with Titanium Dioxide Nanoparticles ..	48
4.5.1 Sample Cleanup on Nanocomposite with Graphitized Carbon Black	50
5 CONCLUSIONS.....	55
6 SOUHRN	56
7 REFERENCES.....	60

ABBREVIATIONS

C14	Tetradecyl
C18	Octadecyl
Da	Dalton
DIOS	Desorption ionization on silicon
GCB	Graphitized carbon black
LDI	Laser desorption/ionization
MALDI	Matrix-assisted laser desorption/ionization
MS	Mass spectrometry
m/z	Mass-to-charge ratio
PLA	Polylactide
ppm	Parts per million
SALDI	Surface-assisted laser desorption/ionization
S/N	Signal-to-noise ratio
TFA	Trifluoroacetic acid
TLC	Thin layer chromatography
TOF	Time-of-flight
UV	Ultraviolet
wt%	Weight percent

LIST OF TABLES

Table 1	Exact masses and partition coefficients of human medicines used as samples in the experiments.....	25
Table 2	Signal-to-noise (S/N) ratio comparison of nanocomposites containing 10% of different nanoparticles. Samples with a concentration of 150 ppm were used.....	34
Table 3	Signal-to-noise (S/N) ratio comparison of nanocomposites with different percentages of nanoparticles. Samples with a concentration of 150 ppm were used.....	36
Table 4	Signal-to-noise (S/N) ratio comparison of nanocomposites containing 10 wt% of titanium dioxide nanoparticles prepared using different techniques. Samples with a concentration of 150 ppm were used.....	38
Table 5	Signal-to-noise (S/N) ratio comparison of different concentrations of model compounds on a stainless steel MALDI plate.....	41
Table 6	Signal-to-noise (S/N) ratio comparison of both top and bottom sides (scratched with sandpaper and unscratched) of different nanocomposites. Samples with a concentration of 10 ppm were used.....	43
Table 7	Signal-to-noise (S/N) ratio comparison of both top and bottom sides (scratched with sandpaper and unscratched) of different nanocomposites. 6 times 0,5 µl of samples with a concentration of 10 ppm were spotted on the surfaces.....	45
Table 8	Comparison of signal-to-noise (S/N) ratios of acebutolol (solution with concentration 150 ppm) collected from three different spots of one sample spot on nanocomposite film containing 10% of titanium dioxide nanoparticles.....	48

1 INTRODUCTION

Mass spectrometry (MS) has become a powerful analytical tool for both qualitative and quantitative analysis for a wide range of applications that is capable of analyzing a variety of compounds from small inorganic molecules to large biomolecules [1].

Matrix-assisted laser desorption/ionization (MALDI) is a soft ionization mass spectrometric method that is important in the analysis of biomolecules and synthetic macromolecules. A sample is mixed with a matrix that facilitates desorption and ionization of the analyte by a pulsed laser beam. The main disadvantage of MALDI is that it is not suitable for the analysis of low molecular weight compounds because the matrix ions produce background that interferes with the analysis of the small molecules [2, 3].

To overcome this problem several matrix-free techniques for laser desorption/ionization have been developed, such as desorption ionization on porous silicon [6], and surface-assisted laser desorption/ionization (SALDI) using sol-gels [8-10], inorganic materials [11], polymeric matrixes [12], high molecular weight matrixes [13], nanostructures [14-20], and carbon allotropes [21-30].

The decreasing reserve of fossil resources and increasing environmental concerns have attracted progressive interest on biodegradable polymers. Polylactide (PLA) is biodegradable aliphatic polyester that can be obtained from renewable resources. This together with its good mechanical properties and thermal plasticity makes PLA an interesting alternative material to common non-degradable polymers for various applications [36].

The goal of this work was to examine other surfaces for SALDI using nanocomposites based on PLA containing nanoparticles such as: halloysite nanoclay, hydroxyapatite, magnesium oxide, montmorillonite nanoclay, silicon dioxide, silicon nitride, titanium dioxide, and graphitized carbon black. Some of these nanoparticles, such as titanium dioxide [11], silicon nitride [20], and GCB [29] have been previously used as surfaces for SALDI. The immobilization of carbon nanotubes improved their properties as a surface for laser desorption/ionization and their applicability [27]. Thus

the incorporation of nanoparticles could confer properties as surfaces for laser desorption/ionization and the use of nanocomposites could make the preparation of both the sample and the surface easier. The use of biodegradable PLA for the nanocomposites has the effect of making these surfaces also environmentally friendly.

2 THEORY

2.1 MASS SPECTROMETRY

2.1.1 Mass Spectrometer

A mass spectrometer is an analytical instrument that separates molecular ions according to their mass-to-charge ratio (m/z) and thus determines the molecular weight of chemical compounds. Ions are produced by losing or gaining electrons. These ions are then separated and detected [2]. A mass spectrometer consists of an ion source that produces ions, a mass analyzer that separates the ions according to their mass-to-charge ratio, an ion detector that counts the ions and measures their abundance, and a computer that stores and processes the data and produces mass spectrum [2, 3].

2.1.2 Matrix-Assisted Laser Desorption/Ionization

Matrix-assisted laser desorption/ionization mass spectrometry (MALDI-MS) is a soft ionization method that is used for the analysis of biomolecules and large synthetic molecules. It was developed by Karas and Hillenkamp in the late 1980s [4].

In MALDI, the sample is dissolved in solution containing small organic molecules, called matrix; the mixture is re-crystallized and then desorbed and ionized by a pulsed laser beam. The amount of matrix used ensures that the number of matrix molecules largely exceeds the number of analyte molecules. Analyte molecules are then diluted by the matrix which prevents them from forming clusters. When pulsed laser beam is directed onto the sample, matrix molecules absorb the laser energy which causes their excitation and vaporization. When the matrix molecules are vaporized they carry some of the analyte molecules with them. During this process the analyte is also ionized with the help of the matrix. The mechanism of ionization is still not exactly understood. Absorption of the laser energy by matrix also minimizes damage and fragmentation of the analyte by the laser pulse [2, 3].

MALDI matrix is a nonvolatile solid compound that absorbs the laser radiation at the laser wavelength [2]. Matrix has to have low enough mass to be sublimable, be stable in vacuum [3], be miscible with the analyte and can co-crystallize with the analyte [5]. It also should not be chemically reactive [3]. Selecting the matrix and preparing the sample are the most important steps in the analysis. They are often empirical procedures. Matrix is selected according to the laser wavelength and the class of compounds analyzed. Aromatic organic acids are often used as matrices. Conjugated aromatic systems absorb the laser energy and the carboxylic group provides proton to the analyte. Common MALDI matrices are for example: α -cyano-4-hydroxycinnamic acid, 3,5-dimethoxy-4-hydroxycinnamic acid, and 2,5-dihydroxybenzoic acid [3].

MALDI is a very important technique in the analysis of biomolecules and synthetic macromolecules. This is due to the fact that MALDI allows desorption and ionization of molecules with molecular weight up to 300 000 Da [2, 3]. It also ensures low or no fragmentation of the sample and is suitable for analysis of heterogeneous samples. Other advantages are high sensitivity and relative tolerance of salts compared to other ionization techniques [2].

On the other side, the use of matrix has inherent disadvantages. MALDI requires proper sample preparation because the co-crystallization of the analyte with the matrix is a complex process that is affected by the composition of the matrix, presence of detergents, electrolytes, and other additives. Co-crystallization does also not produce homogenous crystal structures which causes the occurrence of “hot spots” [5]. MALDI is also not suitable for the analysis of low molecular weight molecules (< 500 Da). The matrix ions have low molecular weight and produce background which interferes with the analysis of small molecules [2].

Ionic liquids have also been used as MALDI matrices [6]. Ionic liquids are salts with melting points below 100°C. They typically consist of a nitrogen- or phosphorus-containing organic cation and a large organic or inorganic anion [7]. The use of ionic liquid matrices can overcome some of the drawbacks of solid matrices. Ionic liquids do not require co-crystallization with the analyte and produce homogenous solutions with the analyte, so the “hot spots” are not formed. Ionic liquid matrices can also be used for the analysis of different groups of compounds and wider ranges of molecular weights.

An example of an efficient ionic liquid matrix is N,N-diisopropylethylammonium α -cyano-4-hydroxycinnamate [6].

MALDI spectra include mostly monocharged ions (proton adduct $[M+H]^+$, sodium adduct $[M+Na]^+$, and potassium adduct $[M+K]^+$), and sometimes also multiply charged ions ($[M+2H]^{2+}$, $[M+3H]^{3+}$), multimers and fragments [3].

2.1.3 Matrix-Free Laser Desorption/Ionization Techniques

Although MALDI is a useful technique for the analysis of a wide range of compounds, it is not suitable for the analysis of small molecules because of the matrix background. To overcome the problems with matrix background in the analysis of small molecules, several matrix-free techniques for laser desorption/ionization (LDI) have been developed, such as desorption ionization on porous silicon [8, 9], and the use of sol-gels [10-12], inorganic materials [13], polymeric matrixes [14], high molecular weight matrixes [15], nanostructures [16-22], and carbon allotropes [23-32]. When a matrix-free method is used, the sample is placed directly onto a surface and analyzed. Mixing with the matrix and co-crystallization are not required [5].

Desorption Ionization on Silicon

The first matrix-free laser desorption/ionization mass spectrometry method developed is called desorption ionization on porous silicon (DIOS) [8]. Porous silicon is prepared from flat crystalline silicon by an etching procedure in which a nanocrystalline surface is formed. Newly etched surfaces are hydrophobic (due to silicon-hydride termination) and can be easily functionalized as required [8]. Porous silicon surface absorbs ultraviolet (UV) light which is then transferred to the analyte trapped on the surface and facilitates desorption and ionization of the analyte. Porous silicon surface also exhibits photoluminescence after exposure to UV light [8]. The pore diameter and shape of the silicon are affected by the preparation conditions and are essential to DIOS performance [9]. DIOS provides little or no fragmentation and little or no background

spectra interference which makes it suitable both for analysis of biomolecules and small molecules.

Sol-gels

Another matrix-free LDI method is the use of sol-gels. Sol-gels are polymeric compounds formed by siloxane backbone (Si-O) that have useful electrical and optical properties [10]. A sol-gel film in which matrix is immobilized is produced by condensation of tetraethoxy silane with 2,5-dihydroxybenzoic acid [11]. Sol-gels can be also made from titanium and zirconium containing compounds. The advantage of titania sol-gel is that it absorbs UV light and thus no matrix molecule needs to be incorporated [12].

Microstructures, Polymers and Nanostructures

Metal or metal oxide particles immobilized in paraffin were used for matrix-free LDI-MS. The size of the particles was typically in the tens of micrometer range. The lowest background noise and highest intensity spectra were acquired when titanium dioxide powder suspended with paraffin was used [13].

For the analysis of small molecules, porous polymer monoliths were used. Poly(butyl methacrylate-co-ethylene dimethacrylate) monolith required higher laser power to desorb/ionize the analyte than what is used with conventional MALDI matrices. In poly(benzyl methacrylate-co-ethylene dimethacrylate) and poly(styrene-co-divinylbenzene) aromatic groups were incorporated which increased the UV absorption and thus less laser power was required to desorb/ionize the analyte and the quality of the spectra was improved [14].

Silicon nanowires are nanostructured materials that were used for matrix-free LDI. They were grown with silane vapor (SiH_4) on gold nanoclusters deposited on silicon wafers as a template. The nanowires can then be further modified by using

silylating reagents. Lower laser energy was required to desorb/ionize small molecules from the silicon nanowires compared to DIOS and MALDI methods. Due to their high surface area and the fluid wicking properties, the silicon nanowires were used as thin layer chromatography (TLC) plate for chromatographic separation [16]. Another nanostructured material used for matrix-free LDI is mesoporous tungsten titanium oxides surface [17]. As surfaces for surface-assisted laser desorption/ionization (SALDI) nanoparticles of gold [18], silver [19], cobalt [20], zinc oxide [21], and silicon nitride [22] have also been used. For example, the silicon nitride nanoparticles provided clean background spectra and were able to desorb/ionize small molecules from a complex matrix, such as urine spiked with the analyte [22].

Carbonaceous materials

The first carbon containing surfaces used for SALDI were graphite particles dispersed in glycerol [23]. Activated carbon particles were used to cover TLC plate on which both TLC separation and SALDI analysis were then performed [24]. Activated carbon has also been used as combined matrix for both solid-phase extraction and laser desorption/ionization [25].

Carbon nanotubes have been used as an effective SALDI surface. They trap the analyte on the surface, strongly absorb UV light and transfer the energy to the analyte. The nanotubes require less laser energy to desorb/ionize the analyte than organic matrices and also provide cleaner background spectra [26]. Their disadvantage is that they are insoluble in most solvents which makes preparation of the sample difficult.

To improve their solubility, the carbon nanotubes were oxidized [27]. By oxidation, carboxyl groups are introduced onto the surface. These carboxyl groups increase the polarity and solubility of the nanotubes and thus facilitate sample preparation. They also provide additional proton source which enhances the efficiency of desorption/ionization of the analytes [27, 28].

Carbon nanotubes have been also immobilized on the target with polyurethane adhesive to prevent them from flying off from the target when hit by a laser pulse. The

carbon nanotubes preserved the properties of an efficient SALDI surface after immobilization and no interference peaks from the adhesive were observed. Also the contamination of the mass spectrometer by the nanotubes was avoided, the time for “hot-spots” searching was reduced, and the analyte signal stability and the signal-to-noise (S/N) ratio were increased which led to enhanced signal reproducibility [29].

Colloidal graphite has been used as SALDI matrix in imaging mass spectrometry. It provided good sensitivity for small molecules and improved reproducibility of imaging compared to conventional MALDI matrices because of fewer “hot-spots” [30]. Graphitized carbon black (GCB) has been used as a medium for both solid-phase extraction and SALDI analysis. GCB particles were efficient as SALDI surface and provided clean background spectra [31]. The efficiency of desorption/ionization of the analytes was further enhanced when oxidized graphitized carbon black particles were used. Due to the presence of carboxylic groups on the surface after the oxidation, the S/N ratios, especially of basic compounds, were increased [32]. The advantage of GCB and oxidized GCB over carbon nanotubes is their lower cost and the fact that they adhere firmly to the stainless steel plate and do not require use of adhesive substances [31, 32].

2.1.4 Time-of-Flight Analyzer

Time-of-flight (TOF) analyzer is commonly used with MALDI ionization. A linear time-of-flight analyzer is one of the simplest mass analyzers. Packets of ions are produced by a pulsed ionization process, or extracted by application of an electrical pulse, and then accelerated from the ion source into a field-free flight tube by the same electrical potential. Since the ions are accelerated with the same amount of energy but have different masses, they move with different velocities. The smaller ions move faster and reach the detector first, the larger ions move slower and reach the detector later. The mass-to-charge ratios are determined from the time it takes the ions to move from the source to the detector [2, 3, 33].

The main advantage of a TOF instrument is the absence of any upper mass limit. Although a major disadvantage is its relatively poor mass resolution which is caused by

flight time distribution of ions with the same m/z ratio. The ions with the same m/z ratio but with different kinetic energies reach the detector at slightly different times which leads to peak broadening. The flight time distribution is affected by the length of the ion formation pulse, size of the volume where the ions are created, and the variation in the initial kinetic energy of the ions [2, 3, 33].

The kinetic energy spread of ions with the same m/z ratio can be reduced by using delayed pulsed extraction. The ions are first formed and allowed to expand in a field-free region. The ions with more initial energy move in the field-free region further towards the detector than the ones with less energy. After a certain time delay, a voltage pulse is applied to accelerate the ions away from the source. The ions with less initial energy have moved a shorter distance away from the target so they receive more energy from the voltage pulse which compensates for the initial energy distribution [3, 33].

An electrostatic reflector is another means to improve the mass resolution. A reflector consists of a series of grids and ring electrodes that create a retarding field which deflects the ions back into the flight tube. The reflector reduces the kinetic energy distribution of the ions with the same m/z ratio. Ions with more energy go deeper into the reflector before they turn around and thus they spend more time in the reflector. Consequently they leave the reflector later than the less energetic ions and thus they reach the detector at the same time. However, the use reflector decreases the sensitivity and introduces a limited mass range [2, 3, 33].

2.1.5 On-Plate Sample Cleanup

Modified porous silicon surface has been used for sample cleanup prior to DIOS analysis [34]. Oxidized porous silicon surface was modified with silylating agents to create a hydrophobic surface. When the sample is spotted onto the modified silicon surface, the analyte adsorbs onto the surface via hydrophobic interactions and the liquid phase containing salts and other hydrophilic contaminants is removed. The analyte is thus extracted from the complex sample. This approach provides a rapid cleanup and enables the analysis of analytes from a complex matrix. These modified silicon surfaces retain DIOS-MS activity and can be directly used for laser desorption/ionization

analysis. Furthermore, silylation of porous silicon improves its stability against oxidation and hydrolysis. The best results in the study were obtained when a pentafluorophenyl-functionalized DIOS chip was used [34].

On-plate desalting and peptide concentration and subsequent MALDI analysis have also been performed on hydrophobic polymer (poly(methyl methacrylate), polystyrene) spots placed at the centers of stainless MADLI plate wells [35]. Digested protein solution was spotted onto the polymer spots and after it dried it was covered with excess matrix solution. Salts were dissolved in the matrix solution and removed from the spot centre to the spot edge while the digested peptides remained concentrated on the hydrophobic polymer centers of the spots. Due to this process, the size of the spot containing the peptides was reduced and thus the S/N ratio and sensitivity of the analysis were enhanced. This method also simplifies the complicated and time-consuming sample preparation process which has to be normally performed. This is especially advantageous for analysis of low abundance proteins since they can be easily lost during the sample preparation. The identification of the low-abundance proteins is also improved by their concentration on the spot of a smaller size. The highest S/N ratio was obtained when the more hydrophobic polymer (polystyrene) was used and when C₆₀ functional group, which absorbs UV laser energy, was introduced into the polymer [35].

2.2 POLYLACTIDE NANOCOMPOSITES

2.2.1 Polylactide

Polylactide (poly(lactic acid), PLA) is a biodegradable aliphatic polyester [36]. Biodegradable means that it degrades at temperatures up to 50 °C within several months to one year. During the degradation, the ester bonds of PLA are hydrolyzed. Enzymes are not required to catalyze the hydrolysis and the degradation products are non-toxic [36]. PLA is a thermoplastic, high-strength polymer and can be obtained from renewable resources [37]. These properties make it an interesting alternative material to common non-degradable polymers in various applications [38].

The monomer, lactic acid (2-hydroxy propanoic acid), contains an asymmetric carbon and thus exists as two enantiomers, L- and D-lactic acid. Lactic acid can be produced by biological and chemical methods [36, 38].

Biologically lactic acid is made by fermentation of carbohydrates using lactic bacteria, mostly the modified strains of the genus *Lactobacillus*. The lactic acid is formed by fermentation as pure L-lactic acid and leads to stereoregular poly(L-lactic acid) with low molecular weight [36, 38]. Biological production of lactic acid is preferred because the carbohydrates used for fermentation are easily obtained from biomasses, such as corn, sugar beet and potatoes which are renewable resources [36].

Chemically produced lactic acid is a racemic mixture of L- and D-enantiomers [36].

PLA can be synthesized from lactic acid by direct polycondensation polymerization in the presence of a catalyst at reduced pressure. The disadvantage is that the PLA has low molecular weight [36]. High molecular weight PLA can be synthesized by azeotropic condensation polymerization [39] that is carried out in an organic solvent, and solid state polymerization [40] where a crystallized polycondensate is heated up to a temperature lower than the melting temperature for further polycondensation. High molecular weight polymer is also obtained by ring opening polymerization [36]. PLA is then produced by polymerization of lactide, a cyclic dimer of lactic acid, which is prepared by depolymerization of low molecular weight PLA [36, 37]. The structure of PLA is shown in Figure 1.

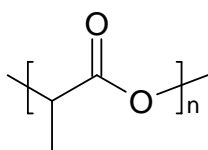


Figure 1. Structure of polylactide

The mechanical properties and crystallinity of PLA are dependent on its molecular weight and stereochemistry [37]. The mechanical properties increase from soft, elastic plastic to stiff, high strength plastic with the increase of molecular weight.

Pure poly(L-lactic acid) is crystalline while poly(DL-lactic acid) is amorphous. Poly(L-lactic acid) also has better mechanical properties due to its more ordered structure [36].

PLA has mostly been used in biomedical and short-term applications [36, 38]. Due to its biocompatibility, biodegradability, and non-toxic degradation products, PLA has been used in many medical applications [36] such as drug delivery systems [41, 42], protein encapsulation and delivery [43], orthopaedic screws [44], development of scaffolds [45], sutures [46], etc. Among its short-term applications are packaging, agriculture and hygiene devices, such as agricultural films, temporary replanting pots, thermoformed trays for fruits and vegetables, degradable rubbish bags, plates, cups, toys, cutlery, etc. [36, 38].

2.2.2 Nanocomposites

Nanocomposites are materials that are obtained by incorporation of nano-sized fillers into a polymer matrix. Nanocomposites are prepared to improve the properties of the polymer [38].

PLA has good mechanical properties and thermal plasticity. However, for certain application it is not as suitable as conventional thermoplastics. In order to improve some of its properties, like flexural properties, gas permeability and thermal stability, and thus extend the range of its possible applications, nanocomposites have been formulated [38].

The main nanofillers used in PLA nanocomposite systems are layered silicate clays (e.g. montmorillonite). The clays have hydrophilic character while PLA is a hydrophobic polymer. To improve the affinity between the clay and the PLA, the clays are modified with ammonium or phosphonium cations with at least one long alkyl chain which increases their hydrophobicity. The resulting clays are called organomodified layered silicates [38].

2.3 DEFINITION OF TERMS

2.3.1 Signal-to-Noise Ratio

Signal-to-noise (S/N) ratio is defined as:

$$S/N = 2H/h$$

where H is the height of the peak and h is the range of the noise [47].

2.3.2 Partition Coefficient

The partition coefficient represents the ratio between the total concentration of a compound dissolved in a hydrophobic solvent (in lipids in an organism) and the total concentration of the compound dissolved in water. The value of the partition coefficient is important for estimating transport and distribution of medicines in the organism. The partition coefficient is measured experimentally in a system where the hydrophobic solvent is octanol and the hydrophilic solvent is water. It is expressed as a logarithm:

$$\log P = c_{\text{octanol}}/c_{\text{water}}$$

where c_{octanol} is the concentration of the compound dissolved in octanol, and c_{water} is the concentration of the compound dissolved in water [48].

The partition coefficient is also used in development of new medicines and in assessment of the drug safety. Very lipophilic medicines accumulate in the lipid-rich regions in the body and thus can cause harm to the organism [48].

3 EXPERIMENT

3.1 CHEMICALS, MATERIALS AND SAMPLES

3.1.1 Water

The water used to prepare solutions was purified by a Millipore water purification system (Millipore Corp., Billerica, MA, USA).

3.1.2 Standards

As model compounds, three human medicines - acebutolol, propranolol and carbamazepine - were used in the experiments. They were purchased from Sigma-Aldrich (St. Louis, MO, USA) in powder form. Stock solutions at a concentration of 2 g/l (2000 ppm) for each substance in methanol were prepared by dissolving the substance in methanol. These stock solutions were further diluted with water solution containing 50% acetonitrile and 0,1% trifluoroacetic acid (TFA) to obtain standard solutions with final concentrations of 0,1 ppm, 1 ppm, 10 ppm, 20 ppm, 50 ppm and 150 ppm. These solutions were used in the experiments and were stored in a refrigerator at 4 °C before use. Figure 2 shows the structures of the three model compounds and Table 1 shows their exact masses and partition coefficients [49].

Table 1. Exact masses and partition coefficients of human medicines used as samples in the experiments

Compound	Exact mass (Da)	Partition coefficient
Acebutolol	336,4	1,7
Carbamazepine	236,3	2,5
Propranolol	259,3	3,0

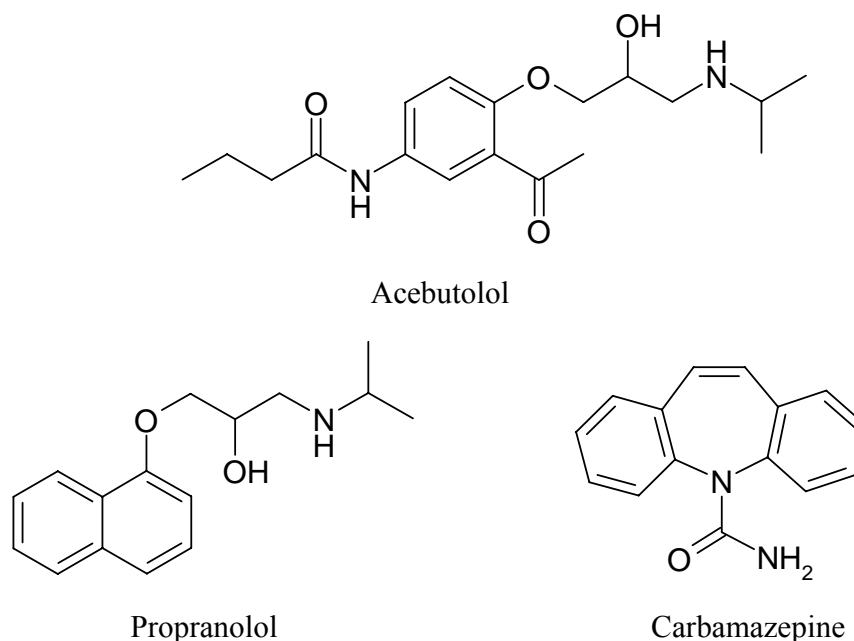


Figure 2. Structures of human medicines used as samples in the experiments.

3.1.3 Other Chemicals

Trifluoroacetic acid (TFA) > 99% purity, acetonitrile, and 25% ammonia solution (all from Sigma-Aldrich, St. Louis, MO, USA) were used for the preparation of the following solutions: 50% acetonitrile and 0,1% TFA solution that was used for diluting of the model compound stock solutions; 1% TFA solution and ammonia solution of concentration 10 mmol/l, both used for on-plate sample cleanup experiment. Methanol (Sigma-Aldrich, St. Louis, MO, USA) was used for dissolving the samples to obtain the stock solutions.

3.1.5 Nanocomposites

Poly(lactide) in pellet form (NatureWorks PLA 5200 D) was obtained from Cargill DOW (Minneapolis, MN, USA) and was used as polymer matrix in the nanocomposites. Graphitized carbon black (particle size < 38 μm , Laboratori Analitici

di Ricerca Associati, Formello, Rome, Italy), hallyosite nanoclay, hydroxyapatite nanopowder $\geq 97\%$ purity (particle size < 200 nm), magnesium oxide 98%, montmorillonite clay (surface modified with 35 – 45% dimethyldialkyl-(tetradecyl(C14)–octadecyl(C18))-amine), silicon dioxide nanopowder 99,5% (particle size 5 – 15 nm), titanium dioxide nanopowder 99,9% (particle size < 100 nm), and silicon nitride (all from Aldrich Chemistry, St. Louis, MO, USA) were used as nanoparticles. Chloroform (HPLC grade) from Fisher Scientific (Waltham, MA, USA) was used to dissolve the PLA.

Nanocomposites contained 5, 10, 20 or 30 weight percent (wt%) of one kind of nanoparticles. A total mass of 5 g (nanoparticles + polylactide) was used for the preparation of a nanocomposite film. Polylactide pellets were dissolved in chloroform; the nanoparticles were added and melt mixed. This mixture was heated up to 40 – 50 °C and stirred for several hours. Then it was spread onto a glass plate to create the film. The film was let dry while chloroform evaporated. The film was removed from the glass plate and placed into a vacuum oven where the remaining chloroform evaporated.

Nanocomposite film containing 10 wt% titanium dioxide nanoparticles was also prepared with the use of an ultrasonic bath. After PLA and nanoparticles were mixed, heated up and stirred, the blend was placed into the ultrasonic bath for 30 minutes to mix more thoroughly and to disrupt nanoparticle clusters. The film was then formed by spreading the mixture onto the glass plate and dried in the same manner as described above.

Another kind of nanocomposite was made with a layer of 10 wt% of titanium dioxide nanoparticles on top. Pure PLA was dissolved in chloroform, heated up to 40 – 50 °C while stirred and after several hours spread onto the glass plate. After 1 hour, two layers of nanoparticles mixed with chloroform were poured onto the top of the PLA film. The film was then dried and chloroform evaporated in the same way as described above.

3.1.4 Urine

Freshly collected human male urine was spiked with propranolol. From the stock solution of propranolol (concentration 2 g/l), volumes of 5 μ l, 10 μ l, and 25 μ l were taken and added to 995 μ l, 990 μ l, and 975 μ l of urine to obtain 1 ml of spiked urine with final concentrations of 10 ppm, 20 ppm and 50 ppm. All urine samples were kept in a refrigerator at 4 °C.

3.2 INSTRUMENTATION

3.2.1 Mass Spectrometry

Positive-ion LDI mass spectra were acquired in reflector mode on a Voyager DE-STR time-of-flight mass spectrometer (Applied Biosystems, Foster City, CA, USA) with a 2,0 m flight tube (3,0 m in reflector mode). A pulsed 337 nm nitrogen laser with a 3 ns pulse width was used for desorption/ionization. The acceleration voltage was set to 20 kV, the grid voltage was 62%, and the delay time was 50 ns.

3.2.2 Software

The data from the mass spectrometer were acquired and processed using Voyager Instrument Control Panel Version 5.10 and Data Explorer Version 4.0.0.0 (both from Applied Biosystems, Foster City, CA, USA). Signal-to-noise (S/N) values were calculated using the automatic S/N calculator in Data Explorer.

3.3 DATA GATHERING

3.3.1 Sample Spotting

From each nanocomposite film, a piece with the size of about 2 cm × 2 cm was cut out, placed onto a modified stainless steel MALDI plate and secured with adhesive tape. To evaluate different surfaces, solutions of the three model compounds with a concentration of 150 ppm were used. Each solution (3 µl) was spotted onto the cut nanocomposite film using an automatic pipette, and let dry. The MALDI plate with the attached nanocomposite was loaded onto the mass spectrometer and SALDI mass spectra were collected. Solutions (3 µl of 150 ppm) of each sample were also spotted onto a stainless steel MALDI plate without addition of any matrix, let dry, and mass spectra were collected in the same way as from the nanocomposites.

In order to determine the lowest concentration of the three model compounds that can still be detected on a stainless steel MALDI plate, solutions with concentrations of 0,1 ppm, 1 ppm, 10 ppm, 20 ppm, and 50 ppm of the compounds were used. 0,5 µl of each solution was spotted onto the MALDI plate and mass spectra were collected without addition of any matrix as described in previous experiments.

To further investigate the surfaces, 3 µl of analyte solutions with concentration of 10 ppm were spotted onto both the top and the bottom side of the nanocomposite film. The surface of the nanocomposites was also scratched with sandpaper and 3 µl of the solutions with concentration of 10 ppm were spotted onto the scratched top and the scratched bottom side of the nanocomposite film as well; and also onto the stainless steel MALDI plate. Spectra were acquired in the same manner as in all other experiments.

In further experiments, 0,5 µl of the model compound solutions with a concentration of 10 ppm was spotted onto the surfaces (onto both the top and the bottom sides, both scratched and unscratched) and onto the MALDI plate and let dry. Another 0,5 µl of the same solution was spotted onto the dry drop and let dry again. The spotting was repeated six times so that the total amount spotted on one spot was 3 µl. Mass spectra were acquired in the same way as in the other experiments.

3.3.2 Data Collection

To obtain SALDI mass spectra, 50 laser shots were accumulated from one spot and averaged. The laser intensity was optimized to obtain the highest signal intensity while fragmentation was as little as possible. Signal-to-noise ratios of proton ($[M+H]^+$), sodium ($[M+Na]^+$) and potassium ($[M+K]^+$) adducts of each of the detected analytes were determined. Mass spectra were acquired from all different nanocomposites and the S/N ratios of all three model compounds were used to compare the nanocomposites as surfaces for SALDI. The spectra were collected from several different spots of each sample spot and the S/N ratios of the most intense signal obtained for each analyte on the surface were used for comparison of the surfaces.

3.3.3 On-Plate Sample Cleanup

Nanocomposites containing 10 wt% of titanium dioxide nanoparticles and 30 wt% of graphitized carbon black (GCB) nanoparticles were used for on-plate cleanup of a complex matrix. A cut nanocomposite film was attached to a modified stainless steel MALDI plate in the same manner as in the other experiments described above. 2 μ l of urine spiked with propranolol to a final concentration of 10 ppm, 20 ppm, and 50 ppm were spotted onto the surface and let dry. The spot was then washed with ammonia solution with concentration of 10 mmol/l. 2 μ l of ammonia solution were spotted onto the urine spot and after 1 minute aspirated back into the pipette. This procedure was repeated three times. After the spot dried, 2 μ l of 1% TFA solution were spotted onto the spot and let dry. As a control, 2 μ l of urine spiked with propranolol to the same concentration as in the experiment were spotted onto the surface and let dry. 2 μ l of 1% TFA solution were spotted onto this spot and let dry. Spectra were acquired from both spots in the same manner as in the experiments described above.

4 RESULTS AND DISCUSSION

4.1 METHOD DEVELOPMENT

The samples in the experiments were spotted onto nanocomposite films where there are no wells like on a regular stainless steel MALDI plate. In order to collect spectra, it is crucial that the sample spot on the film is visible on the screen of the MALDI-MS instrument. Whether the sample spot is visible or not depends on the properties of the nanocomposite. On some of the nanocomposite films the sample spots were well visible while on some of the films they were not visible. This observation was made especially when rough surface and surfaces scratched with sandpaper were used. In that case it was not possible to determine whether the sample spots are within the scope of the screen or not.

To help solve this problem, arrows pointing to the sample spots were made using a permanent pen. However, these arrows were not visible on the screen either. Finally, cuts pointing to the centre of the sample spot were made into the nanocomposite film from two sides (Figure 3). However, when the size of the spot was larger than the screen, which occurred especially on the scratched surfaces, the cuts did not help and it was still difficult to determine where the sample spot is. Improvement was achieved when 0,5 µl of the samples were spotted six times instead of spotting 3 µl once which resulted in smaller sized spots and thus the whole spot with the cuts was visible on the screen which made collecting spectra easier.

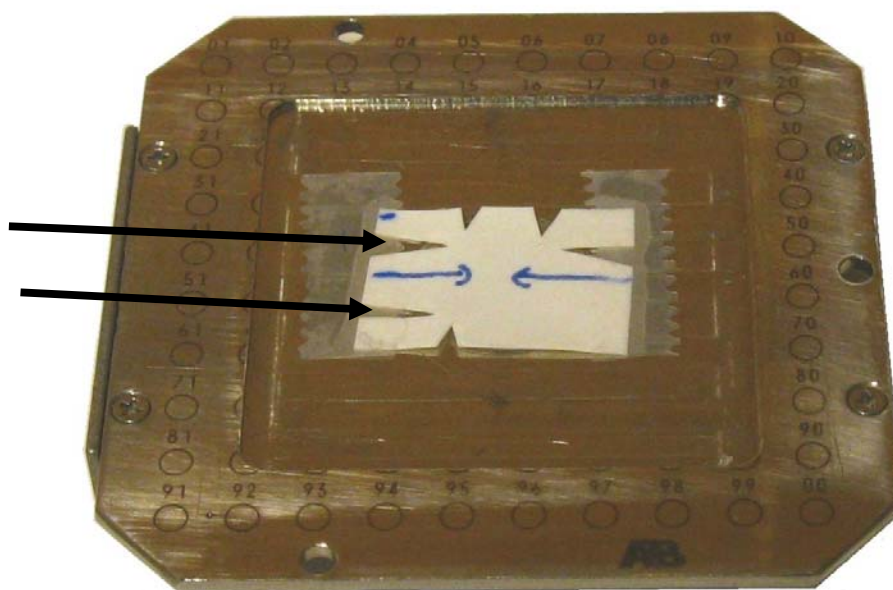


Figure 3. Cut nanocomposite film attached to a modified stainless steel MALDI plate by adhesive tape. Cuts (marked by arrows) pointing to the centers of the sample spots were made on the nanocomposite film to indicate where the sample spots are.

4.2 COMPARISON OF SURFACES

4.2.1 Comparison of Nanocomposites Using 150 ppm Analyte Solutions

Nanocomposites containing 10 weight percent (wt%) of different nanoparticles were compared as surfaces for SALDI. The data obtained from the nanocomposite surfaces were also compared to mass spectra collected from a stainless steel MALDI plate without addition of any matrix (Table 2). The highest signal intensities were obtained from the nanocomposite containing titanium dioxide nanoparticles, where the S/N ratio of proton adduct of acebutolol was 467,2 and the S/N ratio of proton adduct of carbamazepine was 616,5. These values are higher than the ones obtained from the MALDI plate, where the S/N ratio of proton adduct of acebutolol was 280,2 and the S/N ratio of sodium adduct of carbamazepine was 560,4. The S/N ratio of proton adduct of acebutolol obtained from the nanocomposite containing silicon nitride nanoparticles

was 402,4 which is also higher than from the MALDI plate. However, the laser intensities used to acquire spectra from the nanocomposite surfaces were in all three cases higher than the laser intensity used to acquire spectra from the MALDI plate. S/N ratios obtained from all the other surfaces were lower than S/N ratios from the MALDI plate.

Table 2 also shows that the protonated molecules of acebutolol and propranolol gave the most intense signals observed on the stainless steel MALDI plate while the sodium and potassium adducts of carbamazepine provided higher signal intensities than the proton adduct. However, proton adducts of all three compounds provided the highest S/N ratios on all of the nanocomposite surfaces.

Acebutolol and propranolol are basic compounds due to the secondary amino group which both have (structures are shown in Figure 2). Carbamazepine contains an amide group which is only slightly basic and thus carbamazepine is only a very weak base. Carbamazepine contains one more nitrogen, but it is not basic because its free electron pair is part of the conjugated system.

Acebutolol and propranolol are stronger bases and thus bind protons more strongly than carbamazepine. Electrons emitted from the metal surface after laser irradiation then probably neutralize preferentially the proton adducts of carbamazepine because they are less stable than the sodium and potassium adducts. However, the proton adducts of acebutolol and propranolol are stable enough to provide the most intense signals even on the metal plate. No electrons are emitted from the nanocomposites, so the protonated molecules provided the highest signal intensities for all of the compounds.

Table 2. Signal-to-noise (S/N) ratio comparison of nanocomposites containing 10% of different nanoparticles. Samples with a concentration of 150 ppm were used.

Nanoparticles	Acebutolol				Carbamazepine				Propranolol			
	S/N			I	S/N			I	S/N			I
	[M+H] ⁺	[M+Na] ⁺	[M+K] ⁺		[M+H] ⁺	[M+Na] ⁺	[M+K] ⁺		[M+H] ⁺	[M+Na] ⁺	[M+K] ⁺	
GCB	11,5	6,1	12,9	2200	Not detected				Not detected			
Halloysite nanoclay	51,0	8,6		3250	89,2	18,1	11,6	3050	301,1			3100
Hydroxyapatite	51,2	8,5	8,1	3000	164,0	25,2		2800	257,2			2800
Magnesium oxide	45,7			3050	29,5	34,7	51,8	2350	50,2			2200
Montmorillonite nanoclay	40,6	42,3	10,4	2950	112,6	10,9		2950	225,8			3100
Silicon nitride	402,4	33,2	19,7	2750	496,2	275,7	71,7	2750	259,6			3150
Titanium dioxide	467,2	180,4	32,1	2650	616,5	253,3	18,4	2800	73,4			2700
Silicon dioxide	50,4	6,1	5,2	2900	84,0	133,1	20,1	2450	11,3			2400
Steel plate	280,2	10,8	33,3	2400	78,0	560,4	224,5	2400	848,9			2400

I: laser intensity used to acquire the spectra

GCB: graphitized carbon black

4.2.2 Comparison of Nanocomposites with Different Amounts of Nanoparticles

To further investigate the surfaces, nanocomposites containing different percentages of nanoparticles were prepared and compared. As shown in Table 3, the signal intensity did not depend on the amount of nanoparticles in the nanocomposite. The surface with graphitized carbon black (GCB) nanoparticles was the only surface on which higher S/N ratios were obtained from the nanocomposite with higher amount of nanoparticles (30 wt%). The S/N ratio of proton adduct of acebutolol obtained from this nanocomposite containing 30 wt% of GCB nanoparticles was 410,8 which is a higher value than the one acquired from stainless steel MALDI plate. For both silicon nitride and titanium dioxide nanoparticles containing nanocomposites, the highest S/N ratios were obtained when the nanocomposites with 10 wt% of nanoparticles were used. For the nanocomposite containing montmorillonite nanoclay nanoparticles, the highest S/N ratios of acebutolol and propranolol were obtained from the nanocomposite with 10 wt% of nanoparticles, while the highest S/N ratio of carbamazepine was obtained from the nanocomposite with 30 wt% of nanoparticles.

Table 3. Signal-to-noise (S/N) ratio comparison of nanocomposites with different percentages of nanoparticles. Samples with a concentration of 150 ppm were used.

Nanoparticles	wt%	Acebutolol				Carbamazepine				Propranolol			
		S/N			I	S/N			I	S/N			I
		[M+H] ⁺	[M+Na] ⁺	[M+K] ⁺		[M+H] ⁺	[M+Na] ⁺	[M+K] ⁺		[M+H] ⁺	[M+Na] ⁺	[M+K] ⁺	
GCB	10	11,5	6,1	12,9	2200	Not detected				Not detected			
	30	410,8	52,9	78,1	3000	294,9	237,5	63,4	3000	99,5	11,8	13,5	2550
Montmorillonite nanoclay	10	40,6	42,3	10,4	2950	112,6	10,9		2950	225,8			3100
	30	15,1	26,7		2800	346,5	136,2	50,3	3000	33,0			3200
Silicon nitride	10	402,4	33,2	19,7	2750	496,2	275,7	71,7	2750	259,6			3150
	30	72,9	146,7	89,6	2700	122,3	22,7	17,2	2800	21,0			2700
Titanium dioxide	5	113,4	44,1	16,6	2550	60,0	42,7	12,0	2600	73,0	15,0	4,3	2700
	10	467,2	180,4	32,1	2650	616,5	253,3	18,4	2800	73,4			2700
	20	50,4	4,5	10,5	2450	23,0	97,2	32,5	2700	24,4	10,9		2650
	30	63,4	35,8	15,6	2400	79,7	67,1	26,9	2500	61,1			2400
Steel plate		280,2	10,8	33,3	2400	78,0	560,4	224,5	2400	848,9			2400

I: laser intensity used to acquire the spectra

GCB: graphitized carbon black

4.2.3 Comparison of Nanocomposites Prepared Using Different Techniques

As GCB is conductive, the conductivity of the nanocomposite containing GCB nanoparticles was measured. It was found out that the bottom side of the nanocomposite was conductive while the top side was not. It was assumed that the nanoparticles precipitate towards the bottom during the preparation of the nanocomposite films resulting in different properties of the bottom and the top sides of the nanocomposite. Also, since the nanocomposite films were very smooth and shiny, it was assumed that there were no nanoparticles on the surface and that the surface was only made out of the polylactide (PLA) polymer.

To overcome these problems, nanocomposites containing 10 wt% of titanium dioxide nanoparticles were prepared using different techniques. A nanocomposite film was prepared with using an ultrasonic bath while another nanocomposite was made with two layers of nanoparticles on the top. Mass spectra from these surfaces were acquired and compared with nanocomposite containing 10 wt% of titanium dioxide nanoparticles prepared the normal way. Table 4 shows that none of these surfaces provided better results than the ones obtained from nanocomposite with 10 wt% of titanium dioxide nanoparticles prepared using the standard technique.

Table 4. Signal-to-noise (S/N) ratio comparison of nanocomposites containing 10 wt% of titanium dioxide nanoparticles prepared using different techniques. Samples with a concentration of 150 ppm were used.

Titanium dioxide nanocomposite prepared	Acebutolol				Carbamazepine				Propranolol		
	S/N			I	S/N			I	S/N		I
	[M+H] ⁺	[M+Na] ⁺	[M+K] ⁺		[M+H] ⁺	[M+Na] ⁺	[M+K] ⁺		[M+H] ⁺	[M+Na] ⁺	[M+K] ⁺
normal way	467,2	180,4	32,1	2650	616,5	253,3	18,4	2800	73,4		2700
using ultrasonic bath	115,9	18,5	10,2	2600	46,9	133,8	80,7	2650	40,4		2750
with 2 layers of nanoparticles on top	43,9	18,9	5,3	3000	47,0	44,1		2950	22,4	13,1	2600

I: laser intensity used to acquire the spectra

As can be seen in Tables 2, 3, and 4, the surfaces that showed improvement in signal intensity compared to the stainless steel MALDI plate were nanocomposites containing 10 wt% of titanium dioxide nanoparticles, 10 wt% of silicon nitride nanoparticles and 30 wt% of GCB nanoparticles. The signal intensity did not correlate with the percentage of the nanoparticles in the nanocomposite, or with the preparation technique of the nanocomposite.

A reason for this observation could be the uneven distribution of the analytes in the spot on these surfaces which occurs commonly when the “dried droplet” method is used to prepare the spots [50]. The analyte is then found only in some regions of the sample spot, in so called “hot spots”. In the experiments, the search for “hot spots” was probably not performed on all of the surfaces with the same success. For example, the S/N value acquired from a nanocomposite with lower amount of nanoparticles was from a “hot spot”, while the S/N value from a nanocomposite with higher amount of nanoparticles was obtained from a region with a lower amount of the analyte. As a result, the comparison of different nanocomposites using the S/N ratio was difficult.

Another possible explanation of the fact, that there was no correlation between the amount of the nanoparticles in the nanocomposite and the signal intensity; and that the S/N ratios were improved only on a few surfaces compared to a stainless steel MALDI plate, is that there were no or only a few nanoparticles on the surface. The analytes were then desorbed only from the PLA surface with no assistance of the nanoparticles. The three analytes that were used in the experiments were also desorbed from a stainless steel MALDI plate without use of any matrix, so they are assumed to have the ability to be desorbed from surfaces like bare steel plate and PLA.

4.2.4 Comparison of Different Concentrations of Analytes on MALDI Plate

Solutions of acebutolol, propranolol and carbamazepine with concentrations of 0,1 ppm, 1 ppm, 10 ppm, 20 ppm, and 50 ppm were used to determine the lowest concentration that still gave analyte signal on a stainless steel MALDI plate. Mass

spectra were collected without addition of any matrix. For all of the compounds, the lowest concentration detected on the MALDI plate was 1 ppm (Table 5). The signal intensity increased with increasing concentration of propranolol, while for acebutolol and carbamazepine, the higher concentrations did not always provide higher S/N ratios. The highest S/N ratio of acebutolol and carbamazepine was obtained at a concentration of 20 ppm. This was probably again caused by the uneven distribution of the analytes in the sample spots and the fact that no matrix or surface were used to facilitate the analysis.

These three medicines were able to be desorbed and ionized from the stainless steel surface without addition of any matrix because they all contain a conjugated aromatic system (structures are shown in Figure 2) that absorbs the laser energy. All of them are basic compounds so they easily accept a proton. Due to these properties they are assumed to be able to desorb and ionize by themselves without addition of any matrix or surface.

For further experiments, 10 ppm solutions were used. 10 ppm was the lowest concentration that was easily detected for all of the analytes on the MALDI plate. When solutions with the concentration of 10 ppm were used, 10 spectra from different areas within the sample spot with an analyte signal for all of the compounds were obtained while when solutions with the concentration of 1 ppm was used, most of the spectra collected did not contain any analyte signal.

Table 5. Signal-to-noise (S/N) ratio comparison of different concentrations of model compounds on a stainless steel MALDI plate

Concentration	Acebutolol				Carbamazepine				Propranolol			
	S/N			I	S/N			I	S/N			I
	[M+H] ⁺	[M+Na] ⁺	[M+K] ⁺		[M+H] ⁺	[M+Na] ⁺	[M+K] ⁺		[M+H] ⁺	[M+Na] ⁺	[M+K] ⁺	
0,1 ppm	Not detected				Not detected				Not detected			
1 ppm	19,9	14,3	6,8	2500	11,8	63,1	80,2	2400	20,8	5,0		2400
10 ppm	30,1	138,5	106,0	2300	8,1	26,2	29,5	2400	49,7			2400
20 ppm	113,4	167,1	396,3	2300	55,0	232,9	359,4	2400	145,0	17,6	7,3	2400
50 ppm	161,5			2300	27,6	220,4	216,4	2400	229,4	7,3		2300

I: laser intensity used to acquire the spectra

4.2.5 Comparison of Nanocomposites Using 10 ppm Analyte Solutions

Further experiments with solutions of model compounds at 10 ppm were performed to determine if the surfaces facilitate desorption/ionization of the analytes. Since it was assumed that there is only the PLA on the surface of the nanocomposites and no nanoparticles, the surface of the nanocomposites was scratched with sandpaper to remove the layer of the polymer from the surface to ensure that there are some nanoparticles on the surface. Since it was shown that the top side and the bottom side of the nanocomposite film have different properties, mass spectra were collected from both the top and the bottom side of the nanocomposite and also from the scratched top and scratched bottom side of the nanocomposite. Mass spectra were also acquired from a stainless steel MALDI plate and compared. Nanocomposites containing 10 wt% of titanium dioxide nanoparticles (prepared with the use of an ultrasonic bath), 30 wt% of titanium dioxide nanoparticles, and 10 wt% of GCB nanoparticles were used for these experiments.

Table 6 shows that the highest S/N ratios on the surfaces were obtained from scratched bottom side of the nanocomposite containing 10 wt% titanium dioxide nanoparticles prepared with the use of an ultrasonic bath, and scratched top side of the nanocomposite containing 30 wt% titanium dioxide nanoparticles. This means that the scratched surfaces provided better results than the unscratched ones, while it was not obvious whether better results were obtained from the top side or the bottom side of the nanocomposite (about the same number of analyte signals were obtained from both sides). However, all of the surfaces provided significantly lower S/N ratios than the MALDI plate. This could have been caused by the fact that the spot of the sample spreads more on the nanocomposite surface than on the steel MALDI plate which results in a larger size of the spot and thus in lower concentration of the analyte per area unit.

Table 6. Signal-to-noise (S/N) ratio comparison of both top and bottom sides (scratched with sandpaper and unscratched) of different nanocomposites. Samples with a concentration of 10 ppm were used.

Nano- particles (wt%)	Nanocomposite side	Acebutolol				Carbamazepine				Propranolol			
		S/N			I	S/N			I	S/N			I
		[M+H] ⁺	[M+Na] ⁺	[M+K] ⁺		[M+H] ⁺	[M+Na] ⁺	[M+K] ⁺		[M+H] ⁺	[M+Na] ⁺	[M+K] ⁺	
Titanium	top	8,3			2800	Not detected				Not detected			
dioxide	scratched top		18,4	11,3	2800	Not detected				Not detected			
10%	bottom	Not detected				Not detected				Not detected			
UB	scratched bottom	6,9	50,2	119,3	2400	12,9	9,6	4,7	2600	15,5			2400
Titanium	top	Not detected				Not detected				Not detected			
dioxide	scratched top	9,1	8,8	21,3	2400		10,8	4,9	2400	58,2	16,7	7,9	2400
30%	bottom	7,3			2400	Not detected				23,4	6,9		2200
	scratched bottom	Not detected				Not detected				Not detected			
GCB	top	Not detected				Not detected				Not detected			
10%	scratched top	Not detected				Not detected				Not detected			
	bottom		10,6	12,9	2200	Not detected				Not detected			
	scratched bottom	Not detected				Not detected				Not detected			
Steel plate		46,0	332,5	629,4	2400	29,4	541,8	716,2	2500	152,6	12,8		2400

I: laser intensity used to acquire the spectra

UB: prepared with the use of an ultrasonic bath

GCB: graphitized carbon black

To overcome this problem, six times 0,5 μ l of the standard solutions with concentration of 10 ppm were spotted onto the surfaces and onto the MALDI plate instead of spotting 3 μ l, to obtain spot of the same size on all of the surfaces. Nanocomposites containing 10 wt% and 30 wt% of titanium dioxide nanoparticles were used for these experiments.

As shown in Table 7, there was some improvement in the S/N ratios obtained from the nanocomposite surfaces compared to the results when 3 μ l of the solutions were spotted. However, the S/N ratios were still lower than S/N ratios obtained from the MALDI plate. It was also not possible to determine whether the top or the bottom side and the scratched or the unscratched surface provided better results because different results were obtained for different analytes on different surfaces. The highest signal intensities of acebutolol were acquired from the unscratched bottom side of the nanocomposite with 30 wt% of titanium dioxide nanoparticles (S/N=103,9) and from the scratched bottom side of nanocomposite with 10 wt% of titanium dioxide nanoparticles (S/N=96,3). The highest S/N ratios of propranolol were collected from the unscratched bottom side of the nanocomposite with 10 wt% of titanium dioxide nanoparticles (S/N=36,4) and from the unscratched top side of the nanocomposite with 30 wt% of titanium dioxide nanoparticles (S/N=68,0). The highest signal intensities of carbamazepine were obtained from the scratched top side of the nanocomposite with 30 wt% of titanium dioxide nanoparticles (S/N=22,1) and from the scratched bottom side of nanocomposite with 10 wt% of titanium dioxide nanoparticles (S/N=17,6). The only trend that can be seen is that the nanocomposite with 30 wt% of nanoparticles provided slightly better results.

As can be concluded from the results, scratching of the nanocomposite surface with a sandpaper did not improve desorption/ionization of the analytes. The reason could have been that not only the PLA layer but also the nanoparticles were removed by scratching.

Table 7. Signal-to-noise (S/N) ratio comparison of both top and bottom sides (scratched with sandpaper and unscratched) of different nanocomposites. Six times 0,5 µl of samples with a concentration of 10 ppm were spotted onto the surfaces.

Nano- particles (wt%)	Nanocomposite side	Acebutolol				Carbamazepine				Propranolol			
		S/N			I	S/N			I	S/N			I
		[M+H] ⁺	[M+Na] ⁺	[M+K] ⁺		[M+H] ⁺	[M+Na] ⁺	[M+K] ⁺		[M+H] ⁺	[M+Na] ⁺	[M+K] ⁺	
Titanium	top		14,6	10,3	2800	Not detected				8,6			2400
dioxide	scratched top		44,7	14,9	2400	15,9	11,3	2400		16,0	9,2		2400
10%	bottom	9,4	58,1	59,9	2400	Not detected				36,4			2400
UB	scratched bottom	48,0	96,3	77,0	2400	17,8	10,9	2400		14,6	12,0		2400
Titanium	top	25,0	6,8	3,9	2400	5,0		8,3	2600	68,0	51,3	6,6	2400
dioxide	scratched top	Not detected				7,0	22,1	8,8	2800	41,4			2400
30%	bottom	103,9	32,5	11,0	2400	4,3	4,7	5,7	2400	13,0			2400
	scratched bottom	6,6	62,7	93,9	2400	Not detected				Not detected			
Steel plate		160,2	163,0	271,1	2400	6,0	48,5	15,5	2400	198,4			2400

I: laser intensity used to acquire the spectra

UB: prepared with the use of an ultrasonic bath

The smaller size of the sample spots, which was obtained by spotting six times 0,5 μl of the samples instead of 3 μl , made collecting of the spectra easier. On some of the surfaces, the sample spot was not visible on the screen. When the spot was larger than the screen, not even the cuts pointing to the spot were visible on the screen. It was then difficult to determine where the sample spot was when spectra were collected. Since the size of the spot was smaller after spotting six times 0,5 μl of the samples, the whole spot with the cuts was visible on the screen and acquiring of spectra was easier.

4.4 “HOT SPOTS” PROBLEM

Different signal intensities were obtained when spectra were collected from different spots of the sample spot when using the same laser intensity. Three different spectra of acebutolol solution (150 ppm) with different signal intensities recorded from different spots of one sample spot on nanocomposite film containing 10% of titanium dioxide nanoparticles are shown in Figure 4. Table 8 shows S/N ratios of each of the acebutolol adducts in the three spectra.

This was probably observed due to the uneven distribution of the analyte in the spot on these surfaces which occurs commonly when spots are prepared using the “dried droplet” method. Evaporation of the solvent from the sample drop causes a concentration gradient to occur in the drop. A gradient in surface tension, which is caused by the concentration gradient, causes the liquid to flow away from the regions with low surface tension. As a result of this process the analyte is deposited only in some regions of the sample spot, often at the periphery [50].

The occurrence of “hot spots” and the fact that the search for them was probably not performed with the same success on different surfaces made the comparison of these surfaces using S/N ratios difficult.

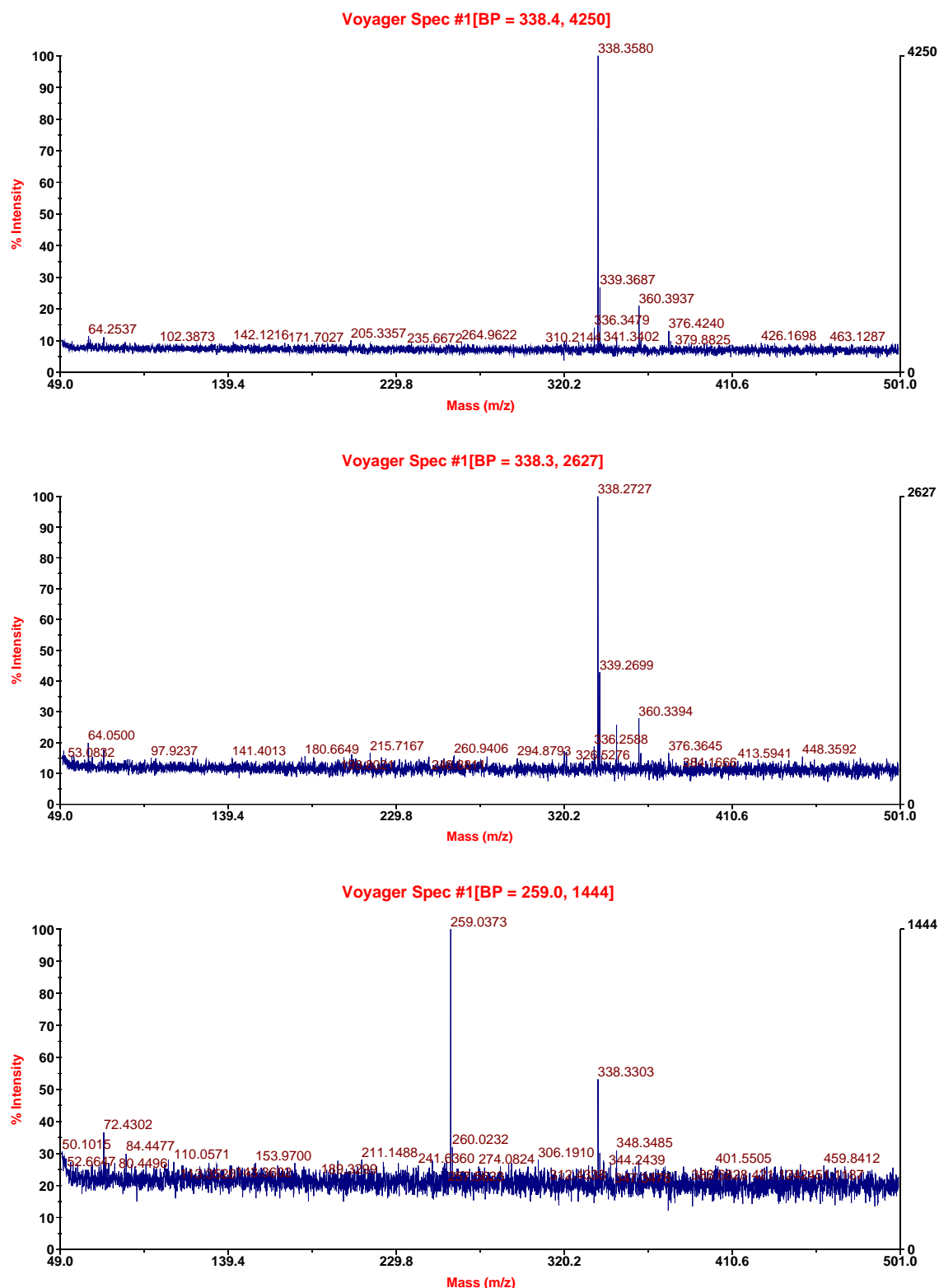


Figure 4. SALDI spectra of acebutolol solution (150 ppm) acquired from three different spots of one sample spot on nanocomposite film containing 10 wt% of titanium dioxide nanoparticles. The peaks at m/z 338, 360 and 376 correspond to proton, sodium and potassium adducts of acebutolol, respectively.

Table 8. Comparison of signal-to-noise (S/N) ratios of acebutolol (solution with concentration 150 ppm) collected from three different spots of one sample spot on nanocomposite film containing 10% of titanium dioxide nanoparticles.

	S/N			I
	$[M+H]^+$	$[M+Na]^+$	$[M+K]^+$	
Spectrum 1	115,9	18,5	10,2	2600
Spectrum 2	71,3	15,3	5,6	2600
Spectrum 3	15,3	5,3		2600

I: laser intensity used to acquire the spectra

4.5 ON-PLATE SAMPLE CLEANUP

On-plate cleanup of a complex matrix was performed on nanocomposites containing 10 wt% of titanium dioxide nanoparticles and 30 wt% of GCB nanoparticles with urine spiked with propranolol to final concentrations of 10 ppm, 20 ppm, and 50 ppm. Propranolol was used to spike urine because it is the most hydrophobic compound out of the three medicines that were used in previous experiments. The hydrophobicity was compared using the partition coefficients. Partition coefficient of propranolol is 3,0 [49]. Propranolol, as the most hydrophobic compound, should adsorb more strongly to the hydrophobic polymer surface of the nanocomposites. As a control, a spiked urine spot that was not washed was used.

4.5.1 Sample Cleanup on Nanocomposite with Titanium Dioxide Nanoparticles

When nanocomposite with titanium dioxide nanoparticles was used for sample cleanup, no propranolol signal was observed, both in the sample spot washed with ammonia solution and in the unwashed control sample spot (Figure 5). Nanocomposite with titanium dioxide nanoparticles as a surface was probably not able to facilitate desorption/ionization of analytes from a complex matrix.

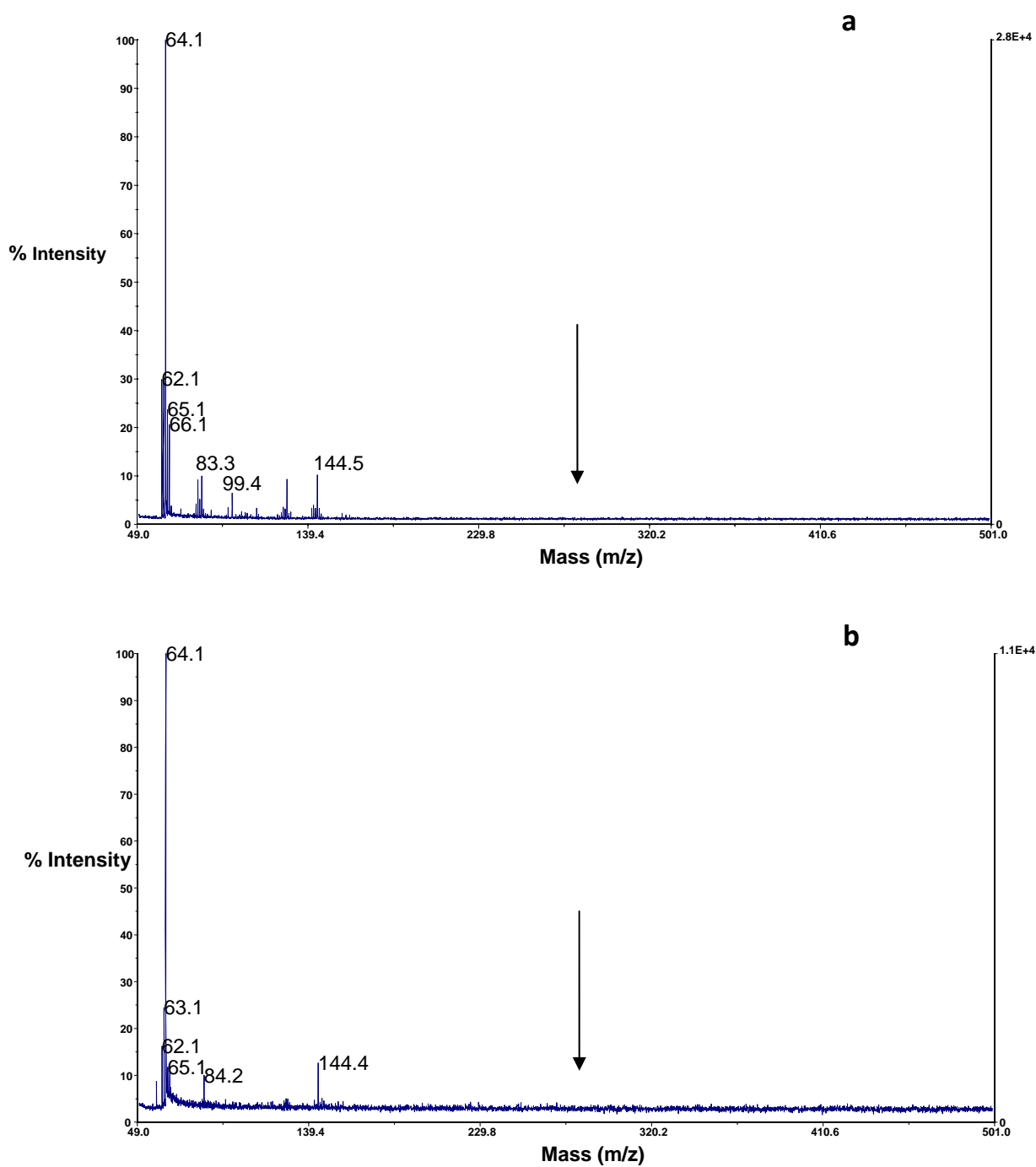


Figure 5. SALDI spectra of urine spiked with propranolol to a final concentration of 50 ppm acquired from nanocomposite film containing 10 wt% of titanium dioxide nanoparticles. No propranolol signal was observed both in **(a)** the unwashed control sample spot and in **(b)** the sample spot washed with ammonia solution. The arrows indicate where analyte signals were expected to show. The laser intensity used to collect the spectra was 2800.

4.5.1 Sample Cleanup on Nanocomposite with Graphitized Carbon Black

When nanocomposite with GCB nanoparticles was used, sodium and potassium adducts of propranolol were detected in both washed sample and unwashed control sample. When urine spiked with propranolol to a concentration of 20 ppm was used, no signal from propranolol was obtained. When the concentration of propranolol in urine was 10 ppm, the S/N ratio of sodium adduct of propranolol acquired from the unwashed control sample spot was 5,9. In the washed sample spot, sodium and potassium adducts of propranolol were detected. The S/N ratio of the sodium adduct was 8,4; the S/N ratio of the potassium adduct was 3,8. The signal intensity was improved when the urine spot was washed with ammonia solution. Also, some of the compounds from urine were removed by the washing process and cleaner spectra were obtained (Figures 6 and 7).

When urine spiked with propranolol to a concentration of 50 ppm was used, the S/N ratios of sodium and potassium adduct from the unwashed sample spot were 20,0 and 13,6, respectively. The S/N ratios of sodium and potassium adduct from the washed sample spot were 12,3 and 4,9, respectively. The washing did not improve the signal intensity, however, the washed urine sample spot provided cleaner spectra compared to the unwashed one (Figures 8 and 9). The analyte was probably removed from the sample spot together with the contaminants by the ammonia solution and that is why the signal intensity of propranolol decreased after the washing.

It was shown that cleaner spectra of a complex matrix sample were obtained after the washing process. However, the signal intensity was only slightly improved and at higher concentrations of the analyte in urine, the S/N ration was decreased. PLA nanocomposite containing GCB nanoparticles could be used as a surface for on-plate sample cleanup prior to SALDI analysis, however, more work is needed to improve the method to obtain better and consistent results.

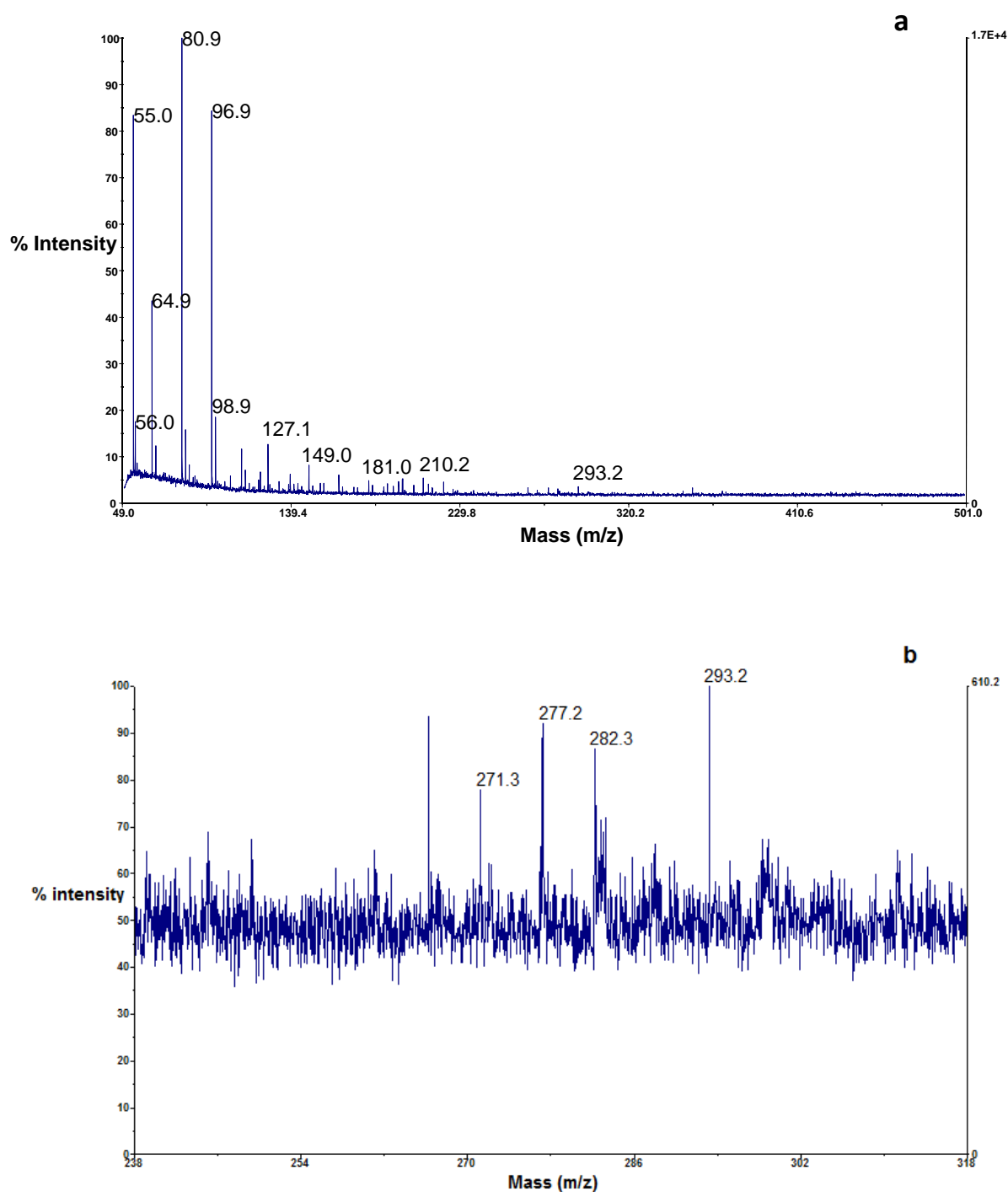


Figure 6. (a) SALDI spectrum of urine spiked with propranolol to a final concentration of 10 ppm acquired from nanocomposite film containing 30 wt% of GCB nanoparticles from the unwashed control sample spot. (b) Zoomed in part of the spectrum showing the sodium adduct of propranolol. The peak at m/z 282,3 corresponds to the sodium adduct of propranolol. The laser intensity used to collect the spectra was 2200.

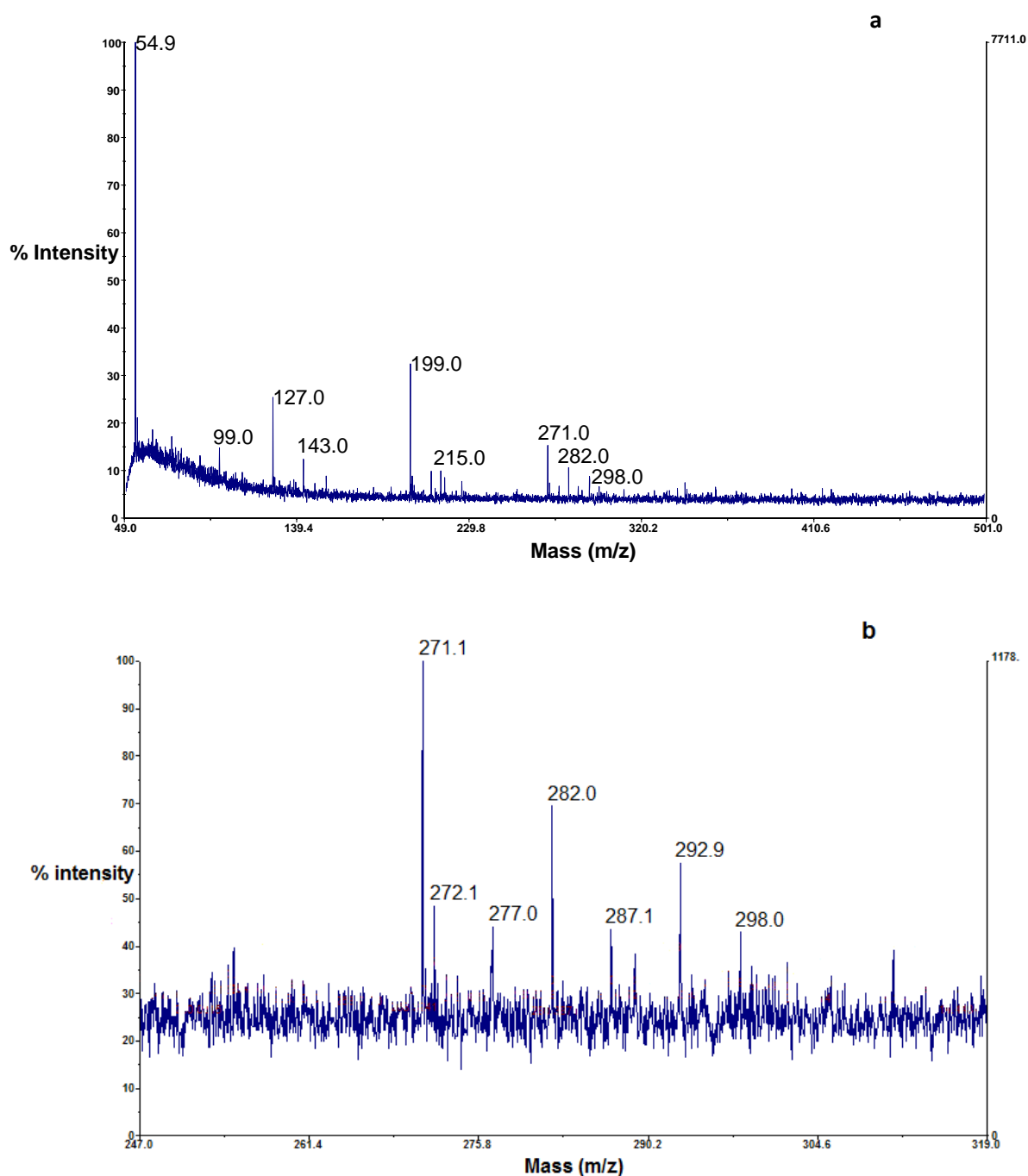


Figure 7. (a) SALDI spectrum of urine spiked with propranolol to a final concentration of 10 ppm acquired from nanocomposite film containing 30 wt% of GCB nanoparticles from the sample spot washed with ammonia solution. (b) Zoomed in part of the spectrum showing sodium adduct of propranolol (m/z 282,0) and potassium adduct of propranolol (m/z 298,0). The laser intensity used to collect the spectra was 2200.

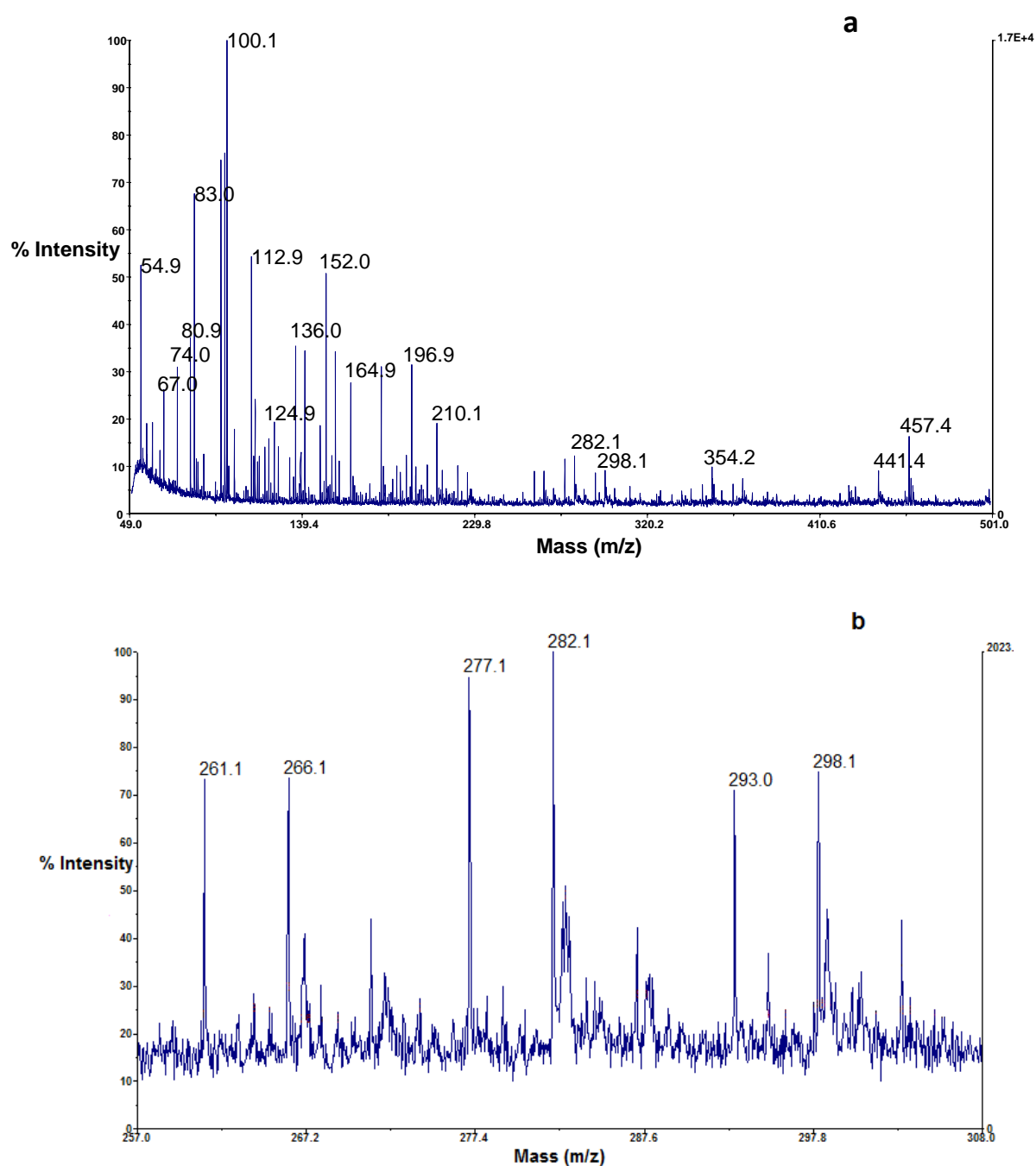


Figure 8. (a) SALDI spectrum of urine spiked with propranolol to a final concentration of 50 ppm acquired from nanocomposite film containing 30 wt% of GCB nanoparticles from the unwashed control sample spot. (b) Zoomed in part of the spectrum showing sodium and potassium adducts of propranolol. The peaks at m/z 282,1 and m/z 298,1 correspond to sodium and potassium adducts of propranolol, respectively. The laser intensity used to collect the spectra was 2200.

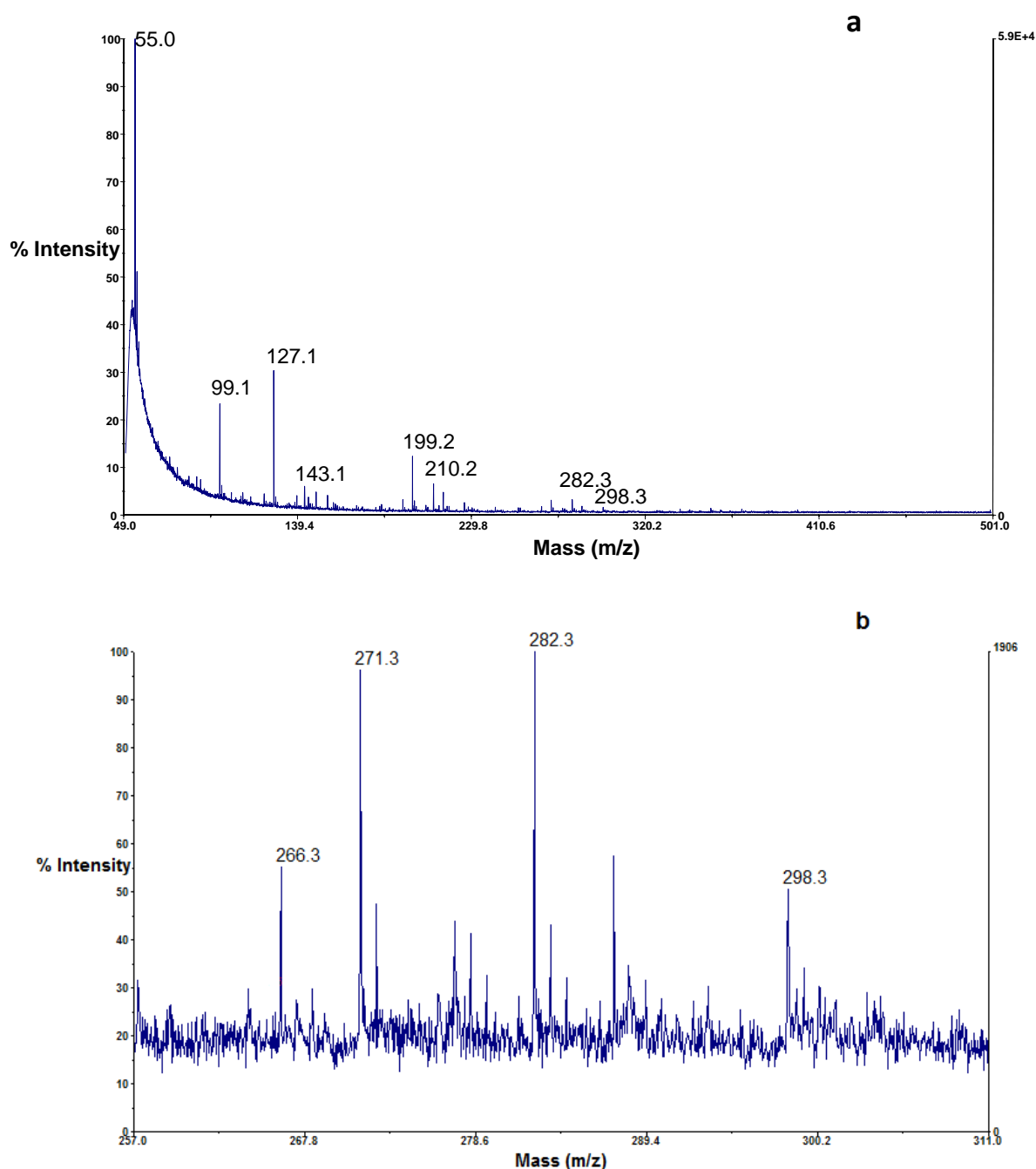


Figure 9. (a) SALDI spectra of urine spiked with propranolol to a final concentration of 50 ppm acquired from nanocomposite film containing 30 wt% of GCB nanoparticles from the sample spot washed with ammonia solution. (b) Zoomed in part of the spectrum showing sodium adduct of propranolol (m/z 282,3) and potassium adduct of propranolol (m/z 298,3). The laser intensity used to collect the spectra was 2200.

5 CONCLUSIONS

Nanocomposites prepared from polylactide and several different kinds of nanoparticles were examined as surfaces for SALDI. Some of the nanocomposites have been shown to be potential surfaces for SALDI; however they were not suitable for the analysis of low concentrations of the analytes. The signal intensities of the analytes were mostly not improved on the nanocomposite surfaces compared to the stainless steel MALDI plate. Nanocomposites containing 30% GCB, 10% silicon nitride, and 10% titanium dioxide nanoparticles can potentially be used as surfaces for SALDI since they provided higher signal intensities than the MALDI plate for some of the analytes in concentration of 150 ppm. However, when the analytes in concentration of 10 ppm were used, the signal intensities obtained from the nanocomposite surfaces were lower than from the MALDI plate. The possible explanations of these observations are that there were no or only a few nanoparticles on the surface of the nanocomposites and that the occurrence of “hot spots” made the comparison using S/N ratio difficult.

It has been demonstrated that the nanocomposite containing GCB nanoparticles could be potentially used as a surface for on-plate cleanup of a complex matrix prior to the SALDI analysis. Cleaner spectra of urine spiked with propranolol were collected after the sample spot was washed on the surface. However, the signal intensity of the analyte was only slightly improved if at all. Further experiments are needed to develop the method so that better and consistent results can be obtained.

6 SOUHRN

Hmotnostní spektrometrie je analytická metoda, která převádí molekuly na ionty, rozděluje je podle jejich poměru hmotnosti a náboje (m/z) a tak určuje molekulární hmotnost chemických látek.

Ionizace laserem za účasti matrice (matrix-assisted laser desorption/ionization, MALDI) patří mezi měkké (šetrné) ionizační techniky hmotnostní spektrometrie a je důležitá zejména pro analýzu biomolekul a syntetických makromolekul. Vzorek je rozpuštěn a smísen s matricí, která absorbuje energii laseru a usnadňuje tak desorpci a ionizaci analytu pomocí laserového pulsu. Použití MALDI však není vhodné pro analýzu látek s nízkou molekulovou hmotností. Matrice, která má také nízkou molekulovou hmotnost, tvoří ionty, které pak interferují s analýzou malých molekul.

Jako řešení tohoto problému bylo vyvinuto několik metod pro ionizaci laserem bez použití matrice. Patří mezi ně desorpce a ionizace na porézním křemíku (desorption ionization on porous silicon, DIOS) a ionizace laserem za účasti povrchu (surface-assisted laser desorption/ionization, SALDI) s využitím polymerních matic, matic s vysokou molekulovou hmotností, anorganických materiálů, sol-gelů, nanostruktur, nanočástic a alotropů uhlíku. Při ionizaci laserem bez použití matrice se vzorek nanese přímo na daný povrch a analyzuje, není třeba ho mísit s matricí.

Polylaktid (kyselina polymléčná, poly(lactic acid), PLA) je biodegradabilní alifatický polyester, který lze získat z obnovitelných zdrojů. Má dobré mechanické vlastnosti a je termoplastický, a proto se jeví jako zajímavý alternativní materiál k běžným nerozložitelným polymerům, který by byl šetrný k životnímu prostředí.

Cílem této práce bylo prozkoumat možnosti využití nanokompozitů složených z polylaktidu a nanočástic halloysitu, hydroxyapatitu, oxidu hořečnatého, montmorillonitu, oxidu křemičitého, nitridu křemičitého, oxidu titaničitého a grafitizovaných sazí (graphitized carbon black, GCB) jako povrchů pro SALDI. Některé z těchto nanočástic byly dříve úspěšně použity jako materiály pro SALDI. Jejich imobilizace v nanokompozitu by mohla usnadnit přípravu povrchu pro

SALDI analýzu a zároveň při použití polylaktidu dát vznik povrchům, které budou šetrné k životnímu prostředí.

Polylaktid byl smísen vždy s jedním druhem nanočástic tak, aby obsah nanočástic ve výsledných nanokompozitech byl 5, 10, 20 a 30 hmotnostních procent. K testování těchto nanokompozitů byly použity standardní roztoky tří léčiv - acebutololu, propranololu a karbamazepinu - v koncentracích 0,1 ppm, 1 ppm, 10 ppm, 20 ppm, 50 ppm a 150 ppm. Kapka vzorku byla nanášena na povrch nanokompozitu, odpařena a analyzována pomocí hmotnostního spektrometru pro MALDI. Výsledné intenzity signálů byly porovnány s intenzitami signálů, které byly získány bez použití matrice z nerezové destičky pro MALDI, pomocí poměru signálu k šumu (signal-to-noise ratio, S/N).

Při použití nanokompozitů s obsahem 10% jednotlivých nanočástic a roztoků léčiv o koncentraci 150 ppm poskytly nejlepší výsledky nanokompozity s nanočásticemi oxidu titaničitého a nitridu křemičitého (Table 2). Intenzity signálů z těchto povrchů byly také jako jediné vyšší než intenzity získané z nerezové destičky.

Vyšší obsah nanočástic v nanokompozitu nevedl u většiny povrchů ke zvýšení intenzity signálu (Table 3). Jedinou výjimkou byl nanokompozit s grafitizovanými saze, kde povrch s obsahem 30% GCB poskytoval výrazně vyšší hodnoty S/N než povrch s obsahem 10% GCB. Tyto hodnoty byly také vyšší než hodnoty získané z nerezové destičky.

Protože byl nanokompozit s grafitizovanými saze vodivý ze spodní strany, zatímco z vrchní strany vodivý nebyl (grafitizované saze jsou vodivé), usoudili jsme, že nanočástice při přípravě nanokompozitu sedimentovali směrem ke spodní straně. Výsledkem byly rozdílné vlastnosti spodní a vrchní strany nanokompozitu. Povrch nanokompozitů byl hladký a lesklý, což nás vedlo k předpokladu, že na povrchu nanokompozitů nejsou žádné nanočástice, ale jenom vrstva polymeru. Jako možné řešení těchto dvou problémů byly připraveny dva nanokompozity obsahující 10% nanočástic oxidu titaničitého, jeden s využitím ultrazvukové lázně v průběhu přípravy a druhý s vrstvou nanočástic na povrchu. Ultrazvuková lázeň by měla zajistit rozrušení shluků a rovnoměrné rozptýlení nanočástic v nanokompozitu.

Takto připravené povrchy však neposkytly žádné zlepšení ve srovnání s povrchem připraveným běžným způsobem (Table 4).

V dalších experimentech byly použity roztoky léčiv o koncentraci 10 ppm. Povrchy tří nanokompozitů - s 10% grafitizovaných sazí a 10% a 30% nanočástic oxidu titaničitého – byly obroušeny skelným papírem, aby se z povrchu odstranila vrstva polymeru a tím se zajistilo, že na povrchu budou nanočástice. Spektra byla potom shromážděna ze spodní i vrchní strany jednotlivých nanokompozitů, z obroušeného i neobroušeného povrchu, a porovnána s výsledky z nerezové destičky. Signál s nejvyšším poměrem signálu k šumu byl získán z obroušené spodní strany nanokompozitu s 10% nanočástic oxidu titaničitého (Table 6). Tyto hodnoty však byly výrazně nižší než hodnoty z nerezové destičky. Důvodem může být fakt, že kapka vzorku se na povrchu nanokompozitu rozptýlí na větší plochu než na nerezové destičce. To vede k vyšší koncentraci analytu na jednotku plochy na nerezové destičce než na nanokompozitu.

Aby se zajistila stejná velikost kapky vzorku na nanokompozitu i na nerezové destičce, bylo nanášeno šestkrát 0,5 μ l vzorku místo jedenkrát 3 μ l na oba druhy povrchů. Intenzity signálů byly zlepšeny oproti předchozím výsledkům, ale byly opět nižší než z nerezové destičky (Table 7). Nejvyšší hodnoty S/N byly získány ze spodní neobroušené strany nanokompozitu s 30% oxidu titaničitého. Nebylo jednoznačné, zda lepší výsledky poskytuje vrchní nebo spodní strana nanokompozitu a obroušený nebo neobroušený povrch, protože výsledky byly různé pro různé nanokompozity a různé analyty. Obroušení povrchu nanokompozitu tedy nezlepšilo desorpci analytu na daném povrchu, možná protože spolu s vrstvou polymeru byly z povrchu odstraněny i nanočástice.

Intenzita signálu také nezávisela na množství nanočástic v nanokompozitu nebo na způsobu přípravy nanokompozitu. Dalším možným vysvětlením, kromě již zmíněného malého nebo žádného množství nanočástic na povrchu připravených materiálů, je nerovnoměrná distribuce analytu v kapce vzorku. Je to běžný jev při nanášení vzorku ve formě kapky a následném odpaření, kdy se po odpaření nachází analyt jenom v některých místech dané kapky a existují tak v rámci jedné kapky místa s vyšší a místa s nižší koncentrací analytu. Je možné, že spektra byla získána z různých povrchů z míst s různými koncentracemi analytů, a proto bylo

porovnávání povrchů pomocí poměru signálu k šumu problematické. Nanokompozity s obsahem 30% GCB, 10% nitridu křemičitého a 10% oxidu titaničitého při použití analytů v koncentraci 150 ppm však zvýšily intenzitu signálu a spolu s faktem, že polylaktid je biodegradabilní a lze ho získat z obnovitelných zdrojů, dělají tyto výsledky z těchto materiálů potenciální povrchy pro SALDI, které by byly šetrné k životnímu prostředí.

Nanokompozit s obsahem 30% grafitizovaných sazí byl také použit pro vyčištění komplexního vzorku – lidské moči s přídavkem propranololu – přímo na daném povrchu. Při čištění vzorku na povrchu je na hydrofobní povrch nanесena kapka vzorku, kapalná fáze obsahující hydrofilní sloučeniny a soli je následně odstraněna, zatímco hydrofobní sloučeniny zůstávají adsorbované na povrchu. Protože je propranolol hydrofobní, měl by se adsorbovat na hydrofobní povrch nanokompozitu. Kapka vzorku moči s propranololem byla nanесena na povrch nanokompozitu, odpařena, vymyta roztokem amoniaku a spektra byla porovnána se spektry z nevymyté kapky. Po vymytí vzorku byla získána čistší spektra, kde bylo snadné identifikovat propranolol (Figure 6, Figure 7, Figure 8, Figure 9). Intenzita signálu propranololu však byla oproti nevymytému vzorku zvýšena jen mírně a při použití vyšší koncentrace propranololu byla snížena. Tyto nanokompozity by tedy mohly být využity k rychlému a jednoduchému vyčištění vzorku před SALDI analýzou. Bude ale třeba provést další experimenty, aby byla tato metoda dále vyvinuta.

7 REFERENCES

1. El-Aneed, A., A. Cohen, and J. Banoub, *Mass Spectrometry, Review of the Basics: Electrospray, MALDI, and Commonly Used Mass Analyzers*. APPLIED SPECTROSCOPY REVIEWS, 2009: p. 210-230.
2. Siuzdak, G., *Mass spectrometry for biotechnology*. 1st ed. 1996, San Diego, USA: Academic Press.
3. Hoffmann, E.d. and V. Stroobant, *Mass spectrometry: principles and applications*. 2nd ed. 2002, Chichester, England: John Wiley & Sons Ltd.
4. Karas, M. and F. Hillenkamp, *Laser desorption ionization of proteins with molecular masses exceeding 10000 daltons*. Analytical Chemistry, 1988: p. 2299-2301.
5. Peterson, D.S., *Matrix-free methods for laser desorption/ionization mass spectrometry*. Mass Spectrometry Reviews, 2007. **26**(1): p. 19-34.
6. Crank, J.A. and D.W. Armstrong, *Towards a Second Generation of Ionic Liquid Matrices (ILMs) for MALDI-MS of Peptides, Proteins, and Carbohydrates*. Journal of the American Society for Mass Spectrometry, 2009. **20**(10): p. 1790-1800.
7. Wasserscheid, P. and W. Keim, *Ionic liquids - New "solutions" for transition metal catalysis*. Angewandte Chemie-International Edition, 2000. **39**(21): p. 3773-3789.
8. Wei, J., J.M. Buriak, and G. Siuzdak, *Desorption-ionization mass spectrometry on porous silicon*. Nature, 1999. **399**(6733): p. 243-246.
9. Shen, Z.X., et al., *Porous silicon as a versatile platform for laser desorption/ionization mass spectrometry*. Analytical Chemistry, 2001. **73**(3): p. 612-619.

10. Schottner, G., *Hybrid sol-gel-derived polymers: Applications of multifunctional materials*. Chemistry of Materials, 2001. **13**(10): p. 3422-3435.
11. Lin, Y.S. and Y.C. Chen, *Laser desorption/ionization time-of-flight mass spectrometry on sol-gel-derived 2,5-dihydroxybenzoic acid film*. Analytical Chemistry, 2002. **74**(22): p. 5793-5798.
12. Chen, C.T. and Y.C. Chen, *Desorption/ionization mass spectrometry on nanocrystalline titania sol-gel-deposited films*. Rapid Communications in Mass Spectrometry, 2004. **18**(17): p. 1956-1964.
13. Kinumi, T., et al., *Matrix-assisted laser desorption/ionization time-of-flight mass spectrometry using an inorganic particle matrix for small molecule analysis*. Journal of Mass Spectrometry, 2000. **35**(3): p. 417-422.
14. Peterson, D.S., et al., *Porous polymer monolith for surface-enhanced laser desorption/ionization time-of-flight mass spectrometry of small molecules*. Rapid Communications in Mass Spectrometry, 2004. **18**(13): p. 1504-1512.
15. Ayorinde, F.O., et al., *Use of meso-tetrakis(pentafluorophenyl)porphyrin as a matrix for low molecular weight alkylphenol ethoxylates in laser desorption/ionization time-of-flight mass spectrometry*. Rapid Communications in Mass Spectrometry, 1999. **13**(24): p. 2474-2479.
16. Go, E.P., et al., *Desorption/ionization on silicon nanowires*. Analytical Chemistry, 2005. **77**(6): p. 1641-1646.
17. Yuan, M.J., et al., *Preparation of highly ordered mesoporous WO₃-TiO₂ as matrix in matrix-assisted laser desorption/ionization mass spectrometry*. Microporous and Mesoporous Materials, 2005. **78**(1): p. 37-41.
18. Su, C.L. and W.L. Tseng, *Gold nanoparticles as assisted matrix for determining neutral small carbohydrates through laser desorption/ionization*

- time-of-flight mass spectrometry*. Analytical Chemistry, 2007. **79**(4): p. 1626-1633.
19. Hua, L., et al., *Silver nanoparticles as matrix for laser desorption/ionization mass spectrometry of peptides*. Journal of Nanoparticle Research, 2007. **9**: p. 1133-1138.
 20. Tanaka, K., et al., *Protein and polymer analyses up to m/z 100 000 by laser ionization time-of-flight mass spectrometry*. Rapid Communications in Mass Spectrometry, 2005. **2**(8): p. 151-153.
 21. Watanabe, T., et al., *Surface-assisted laser desorption/ionization mass spectrometry (SALDI-MS) of low molecular weight organic compounds and synthetic polymers using zinc oxide (ZnO) nanoparticles*. Journal of Mass Spectrometry, 2008. **43**(8): p. 1063-1071.
 22. Shariatgorji, M., N. Amini, and L.L. Ilag, *Silicon nitride nanoparticles for surface-assisted laser desorption/ionization of small molecules*. Journal of Nanoparticle Research, 2009. **11**(6): p. 1509-1512.
 23. Sunner, J., E. Dratz, and Y.C. Chen, *GRAPHITE SURFACE ASSISTED LASER DESORPTION/IONIZATION TIME-OF-FLIGHT MASS-SPECTROMETRY OF PEPTIDES AND PROTEINS FROM LIQUID SOLUTIONS*. Analytical Chemistry, 1995. **67**(23): p. 4335-4342.
 24. Chen, Y.C., J. Shiea, and J. Sunner, *Thin-layer chromatography mass spectrometry using activated carbon, surface-assisted laser desorption/ionization*. Journal of Chromatography A, 1998. **826**(1): p. 77-86.
 25. Chen, Y.C., J. Shiea, and J. Sunner, *Rapid determination of trace nitrophenolic organics in water by combining solid-phase extraction with surface-assisted laser desorption/ionization time-of-flight mass spectrometry*. Rapid Communications in Mass Spectrometry, 2000. **14**(2): p. 86-90.

26. Xu, S.Y., et al., *Carbon nanotubes as assisted matrix for laser desorption/ionization time-of-flight mass spectrometry*. Analytical Chemistry, 2003. **75**: p. 6191-6195.
27. Ren, S.F. and Y.L. Guo, *Oxidized carbon nanotubes as matrix for matrix-assisted laser desorption/ionization time-of-flight mass spectrometric analysis of biomolecules*. Rapid Communications in Mass Spectrometry, 2005. **19**: p. 255-260.
28. Pan, C.S., et al., *Using oxidized carbon nanotubes as matrix for analysis of small molecules by MALDI-TOF MS*. Journal of the American Society for Mass Spectrometry, 2005. **16**(6): p. 883-892.
29. Ren, S.F., et al., *Immobilized carbon nanotubes as matrix for MALDI-TOF-MS analysis: Applications to neutral small carbohydrates*. Journal of the American Society for Mass Spectrometry, 2005. **16**(3): p. 333-339.
30. Zhang, H., S.W. Cha, and E.S. Yeung, *Colloidal graphite-assisted laser desorption/ionization MS and MS_n of small molecules. 2. Direct profiling and MS imaging of small metabolites from fruits*. Analytical Chemistry, 2007. **79**(17): p. 6575-6584.
31. Shariatgorji, M., et al., *mu-trap for the SALDI-MS screening of organic compounds prior to LC/MS analysis*. Analytical Chemistry, 2008. **80**(14): p. 5515-5523.
32. Amini, N., M. Shariatgorji, and G. Thorsen, *SALDI-MS Signal Enhancement Using Oxidized Graphitized Carbon Black Nanoparticles*. Journal of the American Society for Mass Spectrometry, 2009. **20**(6): p. 1207-1213.
33. *TOF fundamentals tutorial*. [cited 2010 19/2]; Available from: <http://www.rmjordan.com/Resources/Tutorial.pdf>.

34. Trauger, S.A., et al., *High sensitivity and analyte capture with desorption/ionization mass spectrometry on silylated porous silicon*. Analytical Chemistry, 2004. **76**(15): p. 4484-4489.
35. Jia, W.T., et al., *Rapid and automatic on-plate desalting protocol for MALD-MS: Using imprinted hydrophobic polymer template*. Proteomics, 2007. **7**(15): p. 2497-2506.
36. Gupta, A.P. and V. Kumar, *New emerging trends in synthetic biodegradable polymers - Polylactide: A critique*. European Polymer Journal, 2007. **43**: p. 4053-4074.
37. Garlotta, D., *A literature review of poly(lactic acid)*. Journal of Polymers and the Environment, 2001. **9**(2): p. 63-84.
38. Bordes, P., E. Pollet, and L. Averous, *Nano-biocomposites: Biodegradable polyester/nanoclay systems*. Progress in Polymer Science, 2009. **34**(2): p. 125-155.
39. Enomoto, K., M. Ajioka, and A. Yamauchi, *Polyhydroxycarboxylic acid and preparation process thereof*, U.S. Patent, Editor. 1994, Mitsui Toatsu Chemicals, Inc.: Japan.
40. Moon, S.I., et al., *Melt/solid polycondensation of L-lactic acid: an alternative route to poly(L-lactic acid) with high molecular weight*. Polymer, 2001. **42**(11): p. 5059-5062.
41. El-Baseir, M.M. and I.W. Kellaway, *Poly(L-lactic acid) microspheres for pulmonary drug delivery: release kinetics and aerosolization studies*. International Journal of Pharmaceutics, 1998. **175**(2): p. 135-145.
42. Hu, Y., et al., *Preparation and drug release behaviors of nimodipine-loaded poly(caprolactone)-poly(ethylene oxide)-polylactide amphiphilic copolymer nanoparticles*. Biomaterials, 2003. **24**(13): p. 2395-2404.

43. Chandy, T., et al., *Development of polylactide microspheres for protein encapsulation and delivery*. Journal of Applied Polymer Science, 2002. **86**(5): p. 1285-1295.
44. Kallela, I., T. Iizuka, and A. Salo, *Lag-screw fixation of anterior mandibular fractures using biodegradable polylactide screws: A preliminary report*. Journal of Oral and Maxillofacial Surgery, 1999. **57**(2): p. 113-118.
45. Zhang, R.Y. and P.X. Ma, *Biomimetic polymer/apatite composite scaffolds for mineralized tissue engineering*. Macromolecular Bioscience, 2004. **4**(2): p. 100-111.
46. Viinikainen, A., et al., *Material and knot properties of braided polyester (Ticron (R)) and bioabsorbable poly-L/D-lactide (PLDLA) 96/4 sutures*. Journal of Materials Science-Materials in Medicine, 2006. **17**(2): p. 169-177.
47. *Czech Pharmacopoeia 2009*, Czech Ministry of Health: Prague, Czech Republic.
48. Hartl, J. and K. Palát, *Farmaceutická chemie I*. 1st ed. 2004, Praha, Czech Republic: Nakladatelství Karolinum. 101.
49. *PubChem Compound*. [cited 2010 19/2]; Available from: <http://pubchem.ncbi.nlm.nih.gov/>.
50. Weidner, S.M. and J. Falkenhagen, *Imaging mass spectrometry for examining localization of polymeric composition in matrix-assisted laser desorption/ionization samples*. Rapid Communications in Mass Spectrometry, 2009. **23**(5): p. 653-660.